Interaction of Tau protein with Microtubules in neural cells

Dissertation

zur Erlangung des akademischen Grades

Doctor rerum naturalium

(Dr. rer. nat.)

Fachbereich Biologie/Chemie der Universität Osnabrück

Vorgelegt von

Jörg Brühmann

Osnabrück, April 2014

"*Des is wia bei jeda Wissenschaft, am Schluss stellt sich dann heraus, dass alles ganz anders war*"

- Karl Valentin

Contents

1 Abstract

The molecular dynamic of tau protein, its interaction with microtubules and the changes in both that appear in pathological conditions are a focus of research to get an insight in neurodegeneration. It is known that tau binds to microtubules by four homologous repeats in its carboxyterminal half. We want to examine tau and especially its repeat regions and their role for microtubule-interaction in living neurons using live cell imaging. We created multiple tau fragments with different numbers of repeats and expressed them in neuronal differentiated PC12 cells as a model for neurons. We performed fluorescence decay after photoactivation experiments by measuring the change of fluorescence intensity over time in the activated region in the middle of cell processes. From this experiments we were able to determine association and dissociation rates of the respective constructs by fitting and modeling approaches. Fluorescence decay increased with decreasing number of repeats. We found that a minimum number of three repeats required for microtubule interaction. This could also be observed in the tip of the processes. Destabilization of microtubules by colchicine increases the mobility of full length tau and microtubule-interacting fragments, while stabilization with epothilone D has no effect. Pseudophosphorylation of tau does not significantly affect the fluorescence decay, but leads to an increase of the dissociation and association rate. Truncation of the carboyxterminus after amino acid 421 - which simulates caspase 3 cleavage of tau - or amino acid 401 leads to a decrease of fluorescence decay indicating increased binding of these fragments to microtubules and a higher dissociation rate of these fragments. Furthermore we could show that overexpression of full length tau in PC12 cells increases the fraction of polymerized tubulin. The stronger binding caspase cleavage fragment shows a similar microtubule stabilization.

2 Introduction

2.1 Neurodegenerative Diseases

Alzheimer's disease (AD) is characterized by a progressive loss of memory and cognitive functions, resulting in severe dementia and massive neuron loss [9]. It is the most well known type of dementia and with the increasing number of elderly people and the trend to prolong human life it moved into the focus of public attention. Not only did it become a study subject for scientific research in the last 50 years, it also evolved into an economic factor for modern day societies [59].
AD has two characteristic hallmarks: The first one is the presence of extracellular amyloid plaques containing the aggregated amyloid precursor protein (APP) peptide fragment Aβ. The second hallmark are the intracellular neurofibrillary tangles (NFTs) composed of hyperphosphorylated tau proteins [31].
Characteristic for AD, like many other neurodegenerative diseases, is a loss of neuronal connections or changes in structural plasticity of neurons in an early

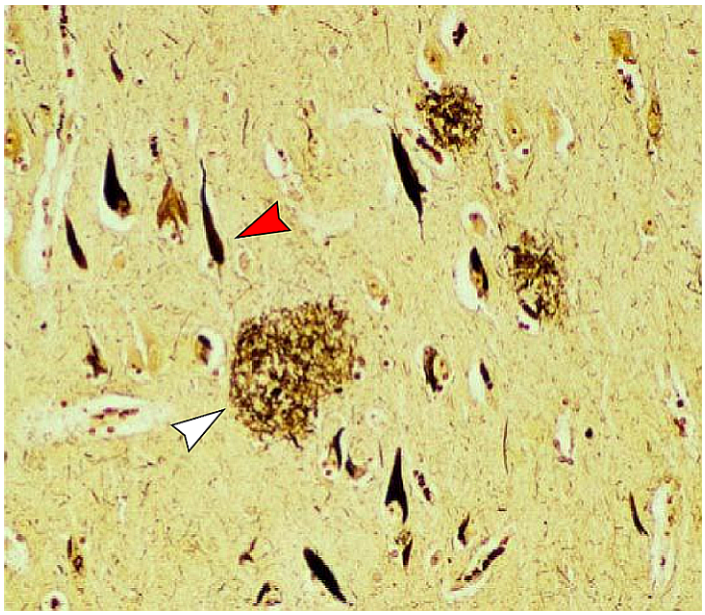

Figure 2.1: **pathology of Alzheimer's disease** Silver stain of an AD patient's cerebral cortex. Amyloid plaques (white arrow) and intracellular neurofibrillary tangles (red arrow) can be visualized. (Chong 2005 [17] *modified*)

stage of disease progression [4]. As well as for Aβ-plaques as for NFTs, a specific pathway of occurrence of pathogenic hallmarks can be observed. They first appear in layer II of the entorhinal cortex. This region projects into the dentate gyrus of the hippocampus, where both NFTs and amyloid plaques can be found in later stages of disease progression, before they are found in limbic and association cortices [18, 21, 51, 67].
Accumulation of hyperphosphorylated Tau protein is also seen in several other human neurodegenerative disorders, called tauopathies. Some of these diseases are Frontotemporal Dementia, Pick disease, Dementia with agyrophilic grains and Cortico-basal degeneration. In all these diseases abnormally hyperphosphorylated tau is associated with neurofibrillary degeneration [37].
In vitro studies have shown that abnormally hyperphosphorylated tau is no longer competent in promoting microtubule assembly or binding to microtubules [2]. Since a proper regulation of microtubule dynamics (assembly and disassembly) is essential for normal cell morphology, functions and viability, malfunction tau can lead to a disorganization of the cytoskeleton and therefore to cell death [68]. What makes AD even more complicated is the yet unknown connection between Aβ and tau [38].

2.2 Cytoskeleton and microtubules

The cytoskeleton is an integral part of every cell. It not only provides the cell with structure and shape by acting as a molecular scaffold, but also plays an important roll in intracellular transport processes. Eukaryotic cells contain three main kinds of cytoskeletal filaments, which are microfilaments, intermediate filaments, and microtubules. For our work, microtubules and their role in a cell's shape and polarity are of special interest. Microtubules are tubular polymers, made up of dimers of α- and β-tubulin. They have a distinct polarity with a (-) and a (+) end, where elongation usually occurs in the (+) end. Microtubules are no rigid structures, but are dynamically unstable, undergoing alternating phases of growth and shrinkage, known as "rescue" and "catastrophe". This dynamic instability can be influenced in multiple ways, either by microtubule affecting substances or by regulating proteins as the microtubule-associated proteins (MAPs). The polarity orientation of microtubules in neurons is dependent of the compartment. While microtubules in axons in both axon and dendrite are parallel, the (+) ends of microtubules in axons are directed to the growth cone, the microtubules and in dendrites they have no uniform polarity orientation - roughly equal proportions are oriented with (+) ends to growth cone or cell body [3]. The

cytoskeleton both establishes and maintains polarity in neurons [71]. The stabilization of microtubules plays an important role in inducing axon formation and therefore in neuronal polarization; Microtubules in axons show an increased stability and pharmacological stabilization of microtubules is observed during axon formation [71, 72]. Of central importance for axon formation and neuronal polarity is the specialized, highly motile cellular compartment at the tips of growing axons, termed growth cone. It is composed of a central region filled with organelles and microtubules and a peripheral, highly dynamic, actin-rich region containing lamellipodia and filopodia [64]. The dynamic state of the neuronal cytoskeleton may have an important role in neuronal degeneration [69]. Many neurodegenerative processes are associated with pathological alterations in the dynamic turnover of intracellular proteins including proteins of the neuronal cytoskeleton [4, 28, 70]. Microtubule loss from axons and dendrites is a key contributor to nervous system degeneration during Alzheimer's disease. Yet the connection between tau hyperphosphorylation and microtubule disintegration is still target for many questions - there is little information [38]. One hypothesis is that tau protects microtubules from being destroyed by various other proteins. A pathological condition in which tau would detach from microtubules would make them vulnerable to such factors [68]. Recently the focus fell on a category of microtubule-severing proteins. These proteins are enzymes that to pull out a tubulin subunit from a microtubule anywhere along its length, and thereby 'cut' it by causing it to break into pieces [38]. The activity of katanin, one of the best studied microtubule-severing proteins, is thought to be regulated by microtubule-bound tau, which protects the microtubule from being accessed by katanin [57]. What makes the whole case more complex is that AD is not only a tauopathy, but also Aβ is playing a role here. Besides that beta amyloid is accumulating in AD patients' brains and prompts tau to hyperphosphorylate, recent studies state that Aβ can also elicit microtubule loss, independent of tau dissociation from the microtubules [38].

2.3 Tau Protein

Tau protein was discovered in the middle of the 1970s and is one of the major and most-studied microtubule-associated proteins of the vertebrate nervous system [55]. The tau proteins are abundant in the central and peripheral nervous system and are expressed in neurons, where they are mainly present and mostly found in the axons of neurons [8, 12]. The molecular characterization of tau has given us a glimpse of the complex and diverse organization and modification of

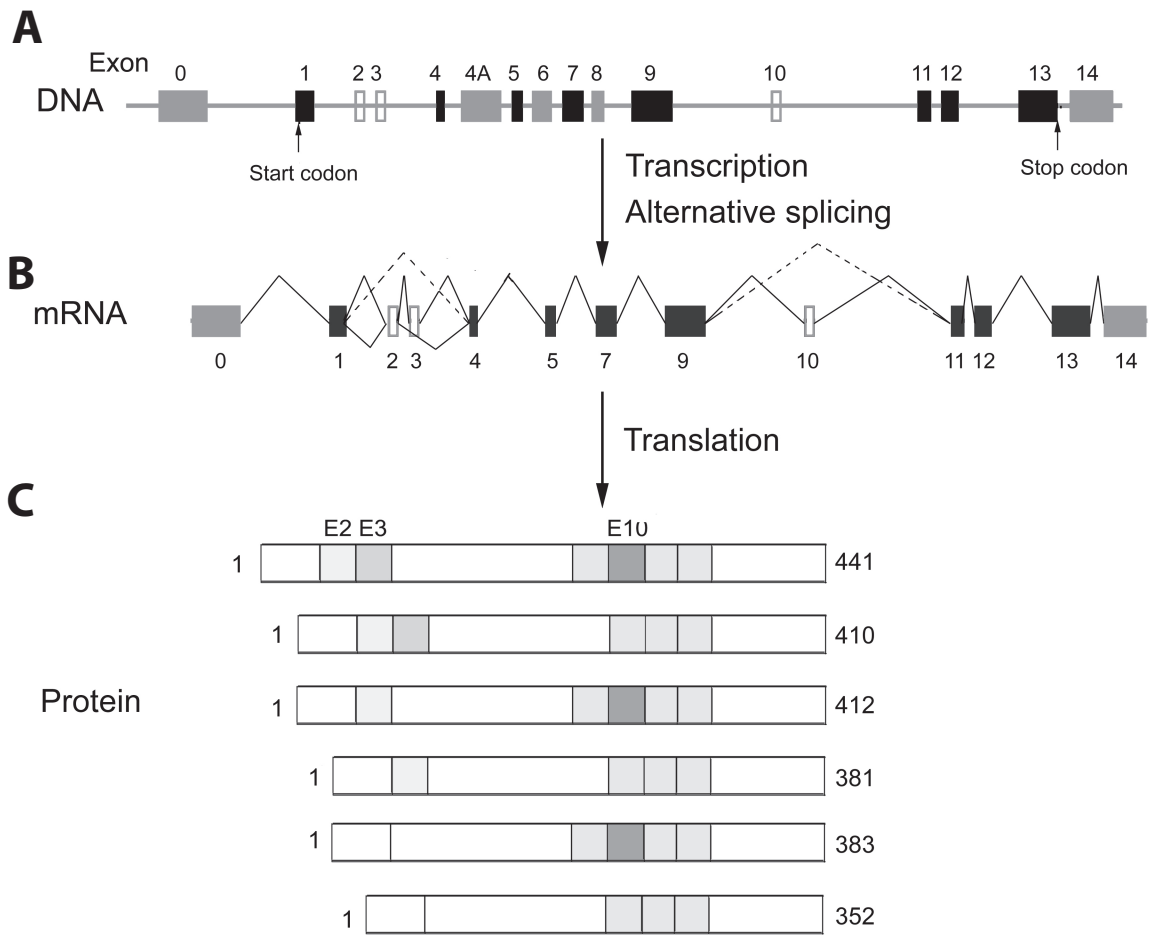

Figure 2.2: **Transcription and translation of tau isoforms**. A total six mRNAs are generated by alternative splicing of exons 2, 3 and 10. **A** the black boxes represent constitutive exons, and the gray and empty boxes represent alternative spliced exons. **B** mRNAs of tau in adult human brain. **C** isoforms of tau in adult human brain. Gray boxes represent the N-terminal inserts (coded by exons 2 and 3) or MT-binding repeats (coded by exons 9, 10, 11 and 12). The second MT-binding repeat coded by exon 10 is highlighted by dark gray box. (*Liu and Gong 2008 [47]*, modified)

the cytoskeleton for tau has been recognized to play major roles in promoting microtubule assembly and stabilizing the microtubules and to maintain the normal morphology of the neurons [30, 42, 61, 68]. In the human central nervous system six different isoforms are generated via alternative splicing of exons 2, 3 and 10 of the human tau gene located on chromosome 17q21 (Figure 2.2) [52]. These isoforms range from 352-441 amino acids and can be distinguished by the absence or presence of two 29 amino acid long inserts in the amino-terminal region and the presence of 3 or 4 repeats in the carboxy-terminal region. The expression of the different isoforms is age dependent: Where the shortest isoform (352

amino acids) can be found during the whole life, the longest isoform (441 amino acids) can only be found in the adult brain [32]. Tau proteins link to microtubules to other cytoskeletal elements or proteins, like neurofilaments and membranous organelles [12, 61]. In neurons, tau is strongly substoichiometric compared with tubulin (~20-40 μM tubulin compared with ~1 μM Tau or less) [19]; in vitro binding studies show saturation at tau:tubulin ratios up to ~0.5, that is about one tau molecule for two tubulin $\alpha\beta$-heterodimers [34].
The overall amino acid composition of full-length tau (441) is unusually hydrophilic. The protein has an overall basic character, although the amino-terminal ~120 residues are predominantly acidic, and the carboxy-terminal ~40 residues are roughly neutral. The amino-terminal region is termed "projection domain", because it projects from the microtubule surface where it may interact with other cytoskeletal proteins or the plasma membrane [10, 36]. It is followed by a part that contains numerous prolines and therefore is names "proline-rich region". The c-terminal half of tau is termed microtubule-binding domain. It contains the repeat region with the already mentioned three to four repeats and a carboxy-terminal part. These highly conserved repeats are 18 amino acid long and separated from each other by less conserved 13-14 amino acid long inter-repeat regions (figure 2.3). It is well documented that the repeat region binds microtubules through a flexible array of distributed weak sites [13, 43]. Nevertheless the exact binding site on microtubules is still unknown and several models for tau binding have been proposed. One model states that the repeat region of tau runs across protofilaments to help stabilize lateral bonds. In this context also the flanking regions - the proline rich region and a proposed R' repeat - play a role by providing stiffening [34, 40, 50]. But also a model was proposed where tau stabilizes microtubules by binding along individual protofilaments [1, 16]. Other studies state that tau is randomly distributed along the outer surface of the microtubules [60].

A number of biophysical studies revealed that physiological tau is an intrinsically unstructured protein, with a very low content of secondary and no tertiary structure [26, 39]. Tau protein can be modified by posttranslational modification. It can be phosphorylated at various sites. There are seventy nine putative serine or threonie phosphorylation sites on the longest brain tau isoforms [12]. Phosphorylation affects tau-microtubule-binding. Microtubule assembly depents partially upon the phosporylation state of tau; Phosphorylated tau proteins are less effective to promote microtubule polymerization than the non-phosphorylated counterparts [45]. Phosphorylation of Ser_{262} for example dramatically reduces the affinity of tau for microtubules in vitro [7]. Tau proteins associated with NFTs are phosphorylated to a greater extent than normal tau [12].

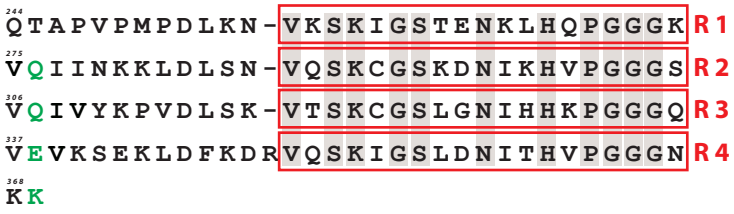

Figure 2.3: **The repeat region of tau consists of 3-4 repeats**. The The repeats (red boxes) are 18 amino acids long and highly homologous (Grey boxes indicate homologous amino acids). They are linked by 13-14 amino acids long inter-repeat regions with a low grade of homology. Green letters indicate truncation mutations (See 4.1.1) (Gustke 1994 [34] *modified*).

Studies show that not only phosphorylation can influence tau protein and its tendencies to form tangles. Also proteolysis can have a massive effect on tangle formation. Caspase 3, a protease that plays a central role in the execution-phase of cell apoptosis cleaves tau after aspartate 421. This truncation leads to a more rapid and extensive assembly of tau into filaments in vitro and is reported in neurons that were treated with amyloid-β peptide in vivo. [27]. Furthermore it was shown that the Asp_{421} truncation fragment is also associated with NFTs in the brains of Alzheimer disease patients [6]. This proteolysis appears to precede the nuclear events of apoptosis, leading to the assumption that Aβ promotes pathological tau filament assembly in neurons by triggering caspase cleavage of tau [27]. In this connection the caspase activation occurs first, followed by tangle formation. It is assumed that caspase cleavage of tau initiates tangle formation and is preceded by truncated tau recruiting normal tau to misfold and form tangles by hours to days [20].

2.4 Live cell imaging

To address questions of protein dynamics, it is important to have a tool that enables us to observe processes in living cells. For this purpose Live cell imaging is an approach to study biological function with high sensitivity.
Fluorescent proteins play a major role in our live cell imaging approaches. The most prominent of them are *green fluorescent protein* (GFP) from the jellyfish *Aequorea victoria* and its variants [65]. Its importance as a marker protein in cellular biology lies in the possibility to fuse it with other proteins and therefore to visualize, track and quantify them [46]. GFP has a molecular weight of 27 kDa and consists of 238 amino acids; an imidazolone ring structure formed

from residues of the three amino acids Ser_{65},Tyr_{66} and Gly_{67} is the actual fluorophore [53]. While inside the jellyfish energy is provided by the protein aequorin, light of specific wavelength is used for excitation of GFP in scientific applications. Wild-type GFP normally exists as a mixed population of a neutral and an anionic phenolates, which produces the major 397-nm and minor 475-nm absorbance peaks. Upon intense illumination of the protein with ultraviolet light, the chromophore population undergoes photoconversion and shifts predominantly to the anionic form, giving rise to an increase in minor peak absorbance (Figure 2.4). This produces an increase in fluorescence of about threefold upon excitation at 488 nm [56]. Substituting Thr_{203} with a histidine results in a mutant that has

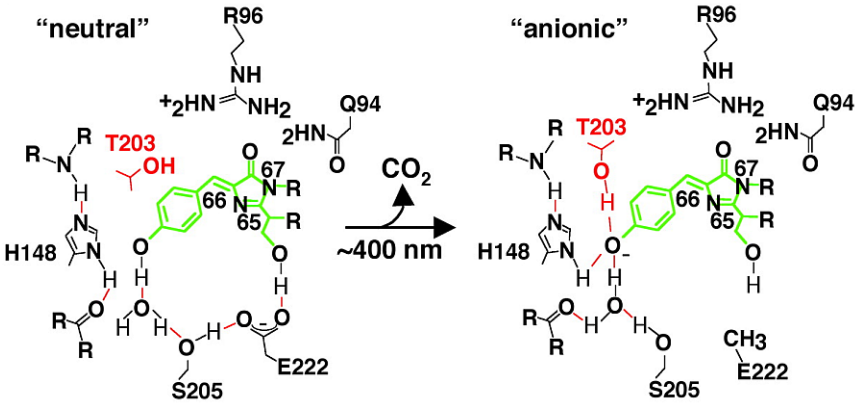

Figure 2.4: Structure of the chromophore of wild-type GFP before (left) and after (right) photoconversion. The neutral phenolic form can be photoconverted into the anionic phenolate form by illumination with UV light. Rotation of the T203 and decarboxylation of glutamic acid 222 (E222) are structural rearrangements that may be the key features for this photoconversion. The green color of the chemical structure indicates the light-emitting structure of the chromophore(Lippincott and Patterson 2002 [56], *modified*).

almost no detectable fluorescence, but photoconversion by irradiation with UV laser light (∼ 400 nm) leads to a 100-fold increase of green fluorescence in the anionic form [48]. The T203H variant therefore serves as a photoactivatable form of GFP, so called PAGFP. The feature of "photoactivatability" is essential: It now is possible to mark small specific populations of tagged proteins inside the cells and track them over time with a Fluorescence Decay After Photoactivation (FDAP) approach. This type of this selective photoactivation produces a population of highlighted proteins more rapidly and with grater optical enhancement than selective photobleaching outside a similar population of GFP molecules. Also, newly synthesized proteins will not be fluorescent, which makes analysis of protein dynamics much less complicated [56].The short time required for photoactivation and the lower intensity of irradiation leads to a lower risk of

phototoxicity [56]. The utility of PAGFP for addressing biological questions was demonstrated in several different experimental setups, for example, the study of embryogenesis, metastasis and tumor formation, or taxis reactions of free unicellular organisms [48].

2.5 Aim of this thesis

This study tries to address the interaction of tau protein with microtubules in living cells. In the first part of this study we characterize changes in the interaction of tau with microtubules by reduction of repeats in the repeat domain of tau. We analyze the mobility of tau and calculate biophysical constants. We also look at local differences by analyzing tip of the process. By using of stabilizing agent Epothilone D and destabilizing agent Colchicine we try to observe alterations in fluorescence decay and association and dissociation rates connected to microtubule stability. In the second part of this study we examine the effect of caspase cleavage and the carboxy-terminal part of tau on the tau-microtubule interaction by looking at caspase cleavage mimicking tau fragments. In the third part we are addressing changes in the degree of tubulin polymerisation caused by expression of human tau protein in our model cell system.

3 Material and Methods

3.1 Material

3.1.1 Devices and Materials

3.1.1.1 Plasticware

All plasticware, if not discribed otherwise, were obtained from following companies:

- Eppendorf AG, Hamburg
- Greiner BioOne GmbH, Frickenhausen
- Milipore GmbH, Schwalbach
- Nunc GmbH & Co KG, Wiesbaden
- Sarstedt AG & CO, Nürmbrecht

3.1.1.2 Glassware

Glassware were obtained from the following companies:

- Brand GmbH & CoKG, Weinheim
- Fisher Scientific GmbH, Schwerte
- Glaswarenfabrik Karl Hecht KG, Sondheim
- Hirschmann Laborgeräte GmbH & Co KG, Eberstadt
- Poulton & Graf GmbH, Wertheim
- Schott Glas, Mainz

3.1.1.3 Devices

Agarose documentation system	MicroDOC gel documentation system (Cleaver Scientific Ltd.,Rugby, UK)
Agarose chamber	Manufactured in the workshops of the Universities of Osnabrück and Heidelberg
Analytic balances	Typ 572 (Kern & Sohn GmbH, Balingen-Frommern), Typ 1702 (Satorius AG, Göttingen)
Centrifuges and rotors	Table top centrifuge Biofuge Fresco, Megafuge 1.0R (Heraeus, Hanau) Sorvall Discovery 90SE with Sorvall Surespin 630 rotor (Thermo Scientific GmbH, Waltham, USA)
Cryo freezing box	Nunc GmbH, Wiesbaden
Cryo tubes	1,8 mlNonclon™(Nunc GmbH, Wiesbaden)
ELISA reader	Emax precicion multi plate reader (Molecular Devices Germany GmbH, Biberach an der Riss)
ECL detection system	Fusion SL (Vilber Lourmat Deutschland GmbH, Eberhardzell)
Freezers and refrigerators	Liebherr Comfort (Liebherr, Biberach an der Riss)
Gas burner	Laborgaz 206 (C.G.I.D. Hatterheim) Fireboy (Tecnomara, Zürich, CH)
Glass bottom cell-culture dish	Glas bottom culture dish P35G-1.0-14-C No. 1.0, uncoated, gamma-irradiated (MatTek Coorporation, Ashland, USA)
Ice machine	Scotsman MF22-AS (Endonis Deutschland GmbH, Herborn)
Incubators	HeraCell (Kendro Laboratory Products GmbH, Langenselbold)
Incubation chamber (LSM)	Solent Scientific Limited, Segensworth, UK
Microscope	Laser Scanning Microscope Nikon Eclipse TE2000-U (Nikon GmbH, Düsseldorf) Optical microscope Leitz Labovert (Leica Microsystems AG, Wetzlar)
Microwave	Proline SM18 (Proline, Korea)

Objective (LSM)	Nikon CFI Plan Apo VC 60X Oil, N.A. 1.4
PCR Thermocycler	MasterCycler gradient (Eppendorf AG, Hamburg)
pH-Meter	Mikroprocessor pH-Meter 761 (Metrohm AG, Herisau CH)
Photometer	Biophotometer (Eppendorf AG, Hamburg) NanoDrop ND-1000 Spectrometer (Thermo Fisher Scientific, Frankfurt a.M.)
Pipettes	Eppendorf 10 µl, 20 µl, 100 µl, 200 µl, 1000 µlwith adjustable volume (Eppendorf AG, Hamburg) Gilson PIPETMAN Classic™2 µl, 10 µl, 20 µl, 200 µl, 1000 µlwith adjustable volume (Gilson, Inc., Middleton, USA)
Pipetting aids	Pipetboy acu (INTEGERA Biosciences GmbH, Fernwald)
Power supply	Power Pac 1000 (Bio-Rad Laboratories GmbH, München)
PVDF transfer membrane	0.45 µm pore size, Immobilion-P (Milipore GmbH, Eschborn)
SDS-PAGE accessories	acrylic glass electrophoresis chambers (Workshops of the University of Osnabrück), glass plates, seperators and combs (Sigma)
Sterile work bench	HeraSafe (Kendro Laboratory Products GmbH, Langenselbold)
Thermomixer	Eppendorf Thermomixer comfort (Eppendorf AG, Hamburg)
Transfection tubes	15 ml(Sarstedt AG & Co KG, Nürnbrecht
Western blot tank	Manufactured in the workshop of the University of Osnabrück

3.1.2 Molecular Biology

3.1.2.1 Plasmids

Plasmid	Source	Resistance
pCMV-PAGFP-htau 352 wt	Carina Weissmann, AG Brandt	Kanamycin

pCMV-PAGFP-htau 441 wt	Jörg Brühmann, AG Brandt	Kanamycin
pCMV-PAGFPx3 wt	Carina Weissmann, AG Brandt	Kanamycin
pET-htau-441A (5xPHP)	Jochen Eidenmüller, AG Brandt	Ampicilin
L22-PAGFP-htau 441wt	Jürgen J. Heinisch	Ampicilin
L22-PAGFP-htau 352wt	Jürgen J. Heinisch	Ampicilin
L22-mCherry-htau 441wt	Jürgen J. Heinisch	Ampicilin
L22-mCherry-htau Δ421	Jürgen J. Heinisch	Ampicilin
L22-3×mCherry	Jürgen J. Heinisch	Ampicilin
L3 helper plasmid	Pavel Osten	Ampicilin
L4 helper plasmid	Pavel Osten	Ampicilin
pIREShyg2_PAGFP-αTubulin	Patricia Wadsworth, UMass Amherst, US	Ampicilin

3.1.2.2 Primers

Primers were all obtained from Biomers.net GmbH (Ulm).

№	Name	Sequence	Tm
1	Δ369	5’-CGTCCCTGGCGGAGGAAATTAAAAGATTG AAACCC-3’	80.4 °C
2	Δ338	5’-CCAGGAGGTGGCCAGGTGTAAGTAAAATC TGAG-3’	109.1 °C
3	Δ307	5’-GGAGGCGGCAGTGTGTAAATAGTCTACAA ACC-3’	108.0 °C
4	Δ276	5’-GGAGGCGGGAAGGTGTAAATAATTAATAA GAAGCTGG-3’	94.4 °C
5	5xPHP-Δ369 STOP-BamHI-BW	5’-CTTGTGGGTTTCGGATCCTTAATTTCCTCCG CCAGGGACG-3’	78.0 °C
6	5xPHP-Δ338 STOP-BamHI-BW	5’-CAAGCTTCTCAGAGGATCCTTACACCTGGCC ACCTCCTGG-3’	78.0 °C
7	5xPHP-Δ307 STOP-BamHI-BW	5’-CCAGCTTCTTATTGGATCCTTACACCTTCCC GCCTCCCGGCTG-3’	80.0 °C
9	peET441-BGLII-FW	5’-CTTTAAGAAGGAGAAGATCTATGGCTGAGC-3’	66.0 °C
10	5xPHP FW	5’-GGGGGCTGATGGTAAAAC-3’	59.0 °C
11	5x PHP BW	5’-CTTGCTCAGGTCAACTG-3’	56.0 °C

3.1.2.3 Bacterial strains

Strain	Gernotype
Escherichia coli **DH5α**	*F*- *fhuA*2 Δ(*argF-lacZ*)U169 *phoA glnV*44 Φ80 Δ(*lacZ*)M15 *gyrA*96 *recA1 relA1 endA1 thi-1 hsdR*17

3.1.2.4 Bacterial culture

Ampicilin stock solution	100 mg/ml in H_2O, sterile filtered
Kanamycin stock solution	30 mg/ml in H_2O, sterile filtered
LB medium	10 g/l Bacto-Tryphon (Difco), 5 g/l yeast extract (Bacto™), 10 g/l NaCl, adjust to pH 7.5 with 1 M NaOH, autoclave
LB agar	add 15 g/l to LB medium and autoclave, let it cool down to 45 °Cand add antibiotics
TfbI	30 mM KOAc, 100 mM RbCl, 10 mM $CaCl_2 \times H_2O$, 15 % Glycerol, adjust to pH 6.0 with 0.2 M acidic acid, add 50 mM $MnCl_2 \times 4H_2O$, adjust pH to 5.8, sterile filtered
TfbII	10 mM MOPS, 10 mM RbCl, 75 mM $CaCl_2 \times H_2O$, 15 % Glycerin, adjust pH to 6.5 with KOH, sterile filtered

3.1.2.5 Restriction endonucleases and DNA modifying enzymes

Restriction endonucleases

BamHI	Fast Digest, 10 U/µl, (Thermo Fisher Scientific - Germany GmbH, Schwerte)
BglII	Fast Digest, 10 U/µl, (Thermo Fisher Scientific - Germany GmbH, Schwerte)

DpnI	Fast Digest, 10 U/µl, (Thermo Fisher Scientific - Germany GmbH, Schwerte)

Other enzymes

CIP (Calf Intestine Phosphatase)	10,000 U/ml, (New England Biolabs, Frankfurt a.M.)
T4-Ligase	40,000 U/ml, (New England Biolabs, Frankfurt a.M.)
Q5® High-Fidelity polymerase	2,000 U/ml(New England Biolabs, Frankfurt a.M.)
Pfu polymerase	native, 100,000 U /ml, (Thermo Fisher Scientific - Germany GmbH, Schwerte)

3.1.3 Cell Culture

3.1.3.1 Eukaryotic cell lines

Name	Source
PC12 Pheochromocytoma cells (Rat)	John A. Wagner, PhD (Boston)
HEK293FT (Human embryonic kidney) cells	Invitrogen

3.1.3.2 Cell culture media

Name	Composition
DMEM all incl.	DMEM with 10% (v/v) Fetal Calf Serum, 5% (v/v) Horse Serum, 1 (v/v) 0.2 M Glutamine, 1% (v/v) Pen-Strep
DMEM complete	DMEM with 10% (v/v) Fetal Calf Serum, 0.2 M Glutamine, 1% (v/v) Pen-Strep, 1% (v/v) MEM NEAA, 1% (v/v) Sodium Pyruvate
DMEM 1%	DMEM with 0.67% (v/v) Fetal Calf Serum, 0.33% (v/v) Horse Serum, 1 (v/v) 0.2 M Glutamine, 1% (v/v) Pen-Strep
G418	50 mg/ml in ddH_2O, PAA (Pasching, A)

Laminine	50 µg/ml in 0.05 M Na_2CO_3 buffer, Millipore (Eschborn)
NB/B27 medium	NB with 1% (v/v) B27, 1% (v/v) Fetal Calf Serum, 1% (v/v) Horse Serum, 1% (v/v) Glutamine, 100 µg/µl primocine and 25 µM β-mercaptoethanol

3.1.3.3 Stock solutions for cell culture

Name	Source or composition
B27	B27 Serum-Free Supplement (Life Technologies)
β-Mercaptoethanol	MERCK-Schuchardt (Hohenbrunn)
Colchicine	Sigma Aldrich Chemie GmbH (Steinheim)
Collagen	From a preparation of rat tails with 20 mM acetic acid, diluted to 50 µg/ml, sterile filtered
Discodermolide	Amos B. Smith III, University of Pennsylvania
DMEM	Dulbecco's Modified Eagle Medium (High Glucose), sterile filtered (Life Technologies)
Epothilone D	Amos B. Smith III, University of Pennsylvania
HBSS	Hank's Balanced Salt Solution (Life Technologies)
MEM	Minimum Essential Medium Eagle (Sigma Aldrich Chemie GmbH, Steinheim)
MEM NEAA	100× MEM Non-Essential Amino Acids Solution (Life Technologies)
Nerve Growth Factor (NGF)	100 µg/µl mouse NGF (7S) in DMEM without phenole red
NB	Neurobasal Medium (Life Technologies)
Nocodazole	Sigma Aldrich Chemie GmbH (Steinheim)
OPTIMEM	Opti-MEM I Reduced Serum Medium (Life Technologies)
Paclitaxel / Taxol	Sigma Aldrich Chemie GmbH (Steinheim)
1x PBS	8 g NaCl, 0.2 g KCl, 0.2 g KH_2PO_4, 1.15 g Na_2HPO_4, fill with ddH_2O to 1 l, adjust pH to 7.4
Pen-Strep (100×)	PAA Laboratorium GmbH, Pasching
Poly-L-Lysine	100 µg/µl Poly-L-lysine in borate buffer pH 8.5
Primocin	500 mg Primocin (Invivogen, Toulouse, France)
Sodium Pyruvate	100 mM Sodium Pyruvate (Life Technologies)

Vinblastine sulfate salt	Sigma Aldrich Chemie GmbH (Steinheim)

3.1.4 Buffers and Solutions

3.1.4.1 Biochemistry

Name	Composition
APS	10% (w/v) Ammonium persulfate in ddH_2O
Blocking solution	5% (w/v) powdered milk in 1x TBS/Tween
Borate buffer	1.24 g borate, 1.9 g borax (Na-Tetraborate), fill up to 400 ml with ddH_2O, pH 8.5
10× Electrophoresis buffer	30 g Tris, 114 g glycerol, 10 g Sodium dodecyl sulfate (SDS), fill up to 1 l with ddH_2O
ECL solution	ECL-Kit (Thermo Fisher Scientific, Bonn)
4× Lower-Tris	1.5 M Tris/HCl, pH 8.8, 0.4% (w/v) SDS
5× Laemmli buffer	300 mM Tris/HCl, pH 6.8, 10% (w/v) SDS, 50% (v/v) Glycerol, 10% (v/v) ß-Mercaptoethanol, 0.005% (w/v) Bromphenole blue
Lysis buffer	48.9% (v/v) 2x RIPA buffer, 48.9% (v/v) ddH_2O, 2% (v/v) 1 mg/ml Pepstatin, 1% (v/v) 2 mg/ml Leupeptin, 1% (v/v) 0.2 M PMSF, 0,002% (v/v) 0.5 M EDTA
Protein ladder	PageRuler™Prestained Protein Ladder (Fermentas, St. Leon-Rot), 10-250 kDa
2× RIPA buffer	100 mM Tris/HCl pH 7.5, 300 mM NaCl, 2 mM EDTA, 2% NP40, 1% DOC, 0.2% SDS in ddH_2O
TBS/Tween	0.05% (v/v) Polyethylene Sorbitan Monolaurate (Tween 20) in 1x TBS
TEMED	N,N,N,N'-tetramethylethylendiamine
Transfer buffer	0.2 M Glycerol, 250 mM Tris, 20% (v/v) Methanol
4× Upper-Tris	0.5 M Tris/HCl, pH 6.8, 0.4% (w/v) SDS

3.1.4.2 Molecular biology

Name	Composition
Agarose gel	1% (w/v) in 1× TBE
DNA ladder	GenRuler™1kb DNA Ladder, ready-to-use (Fermentas, St. Leon-Rot)

dNTP mix	2 mM, Fermentas (St. Leon-Rot)
EB buffer	Qiagen (Venlo, NL)
Ethidium bromide stock solution	25 mg/ml in ddH_2O
Buffer for Fast Digest Enzymes	5× Green Buffer (Fermentas, St. Leon-Rot)
Ligation buffer	10× T4 Ligase buffer (New England Biolabs, Frankfurt a.M.)
Polymerase buffer	10× Pfu polymerase buffer with $MgSO_4$ (Fermentas, St. leon-Rot)
Quick Solution	Stratagene (La Jolla, USA)
5× TBE	0.45 M Tris, 0.45 M boric acid, 1 mM EDTA, adjust to pH 8

3.1.5 Transfection Reagents and Kits

Name	Source
QIAprep spin Miniprep Kit	QIAGEN (Venlo, NL)
QIAquick Gel Extraction Kit	QIAGEN (Venlo, NL)
Lipofectamin™2000	Invitrogen (Darmstadt)
TransIT®Transfection Reagent	Mirus Bio LCC (Madison, USA)
Pierce BCA Protein Assay Kit	Thermo Scientific Germany GmbH (Schwerte)

3.1.6 Antibodies

Primary Antibodies

Name	Species	Source	Cocentration
anti GFP	Mouse	CloneTec	1:3000
anti GFP	Chicken	Aves Labs Inc.	1:6000

Secondary Antibodies (Tagged to HRP)

Name	Species	Source	Cocentration
antiMouse	Goat	Jackson ImmunoResearch	1:20000
antiChicken	Donkey	Jackson ImmunoResearch	1:20000

3.1.7 Software

Cloning and DNA management	Clone Manager (Sci-Ed Software)
ECL documentation	FusionCapt Advance (Vilber Lourmat Deutschland GmbH, Eberhardzell)
Image processing	Adobe Illustrator CS3, Fiji (a distribution of ImageJ by Wayne Rasband, National Institute of Health, USA), Inkscape, GIMP 2.0
Microscope	EZ-C1 Silver Version 3.91 build 889, NSI-Elements (Nikon)
Statistics	Origin Pro 8.0 (OriginLab)

3.2 Methods

3.2.1 Methods of Molecular Biology

3.2.1.1 Generation of Ψ-competent Cells

For transformation of DNA (see 3.2.1.2) cells are needed that are capable of taking up plasmids. We use a *E.coli*-strain, DH5α for this. They are able to take up plasmids and amplify them very effectively. Preparations were done using the following protocol.

Protocol: A small amount of DH5α cells were transferred to 5 ml LB Medium and incubated on a shaker at 37 °C over night. This pre-culture was then transferred to 100 ml of LB medium and incubated at 37 °C on a shaker. The optical density at 600 nm (OD_{600}) was checked regularly until it reached a value of 0.5. The cells where cooled on ice and transferred to a 50 ml tubes and centrifuged for 10 minutes at 4000 ×g and 4 °C. The supernatant was discarded and the pellets were resuspended and reunified in a total of 80 ml of TfbI buffer. Then the cells were incubated on ice for 5 minutes. Afterwards they were centrifuged for 10 Minutes at 4000 ×g and 4 °C. The supernatant was discarded and the pellet was resuspended in 5 ml TbfII buffer. The cells then where aliquoted to 100 µl each, shock frozen in liquid nitrogen and stored at -80 °C.

3.2.1.2 Transformation and Preparation of DNA

In molecular biology transformation is the process of plasmid-DNA uptake from the surrounding medium by bacterial cells. This method uses the cell's synthesis machinery to amplify DNA in a very simple and effective manner. For the selection of successfully transformed cells the plasmids contain a resistance gene. Afterwards, the DNA can be isolated from the respective cells.

Protocol: 1 µl DNA was added to 100 µl for freshly thawed competent DH5α cells. The cells where incubated on ice for 30 minutes, then a heat shock was applied by incubating the cells at 42 °C for 1 minute. After 2 minutes on ice 900 µl LB medium was added and the cells where incubated at 37 °C for 45 minutes (for ampicilin-resistance) or 90 minutes (for kanamycin-resistance). The cells where spun down at 10000 ×g for 5 minutes and the supernatant was discarded. The pellet was resuspended and transferred to an agar plate containing 1% of the respective antibiotic. The plates where incubated for 16 hours at 37 °C.

After that colonies where picked from the plates and transferred to tubes containing 5 ml LB medium and 1% of the respective antibiotic. These tubes where incubated on an shaker or roller for 16 hours at 37 °C.
The DNA was isolated using the QIAprep miniprep kit according to the manufacturer's manual.

3.2.1.3 Quantification of DNA

DNA was quantified by measuring a 1:70 dilution in a photometer or directly by using a NanoDrop (by courtesy of the biophysics department). The concentration was measured at a wavelength of 230 nm.

3.2.1.4 Restriction of DNA

Restriction enzymes cut DNA on defined sites according to the sequence. This can be of use for the analysis of DNA on the one hand, and for cutting out defined DNA sequences on the other. A wide variety of restriction enzymes gives a lot of possible combinations.

Protocol: The amount of enzyme and respective buffer was chosen according to the manufacturer's manual and the amount of used DNA. Enzymes and buffers were all purchased from Fermentas (St. Leon-Rot). The restriction samples were incubated at 37 °C, the time was dependent of the amount of used DNA. When DNA fragments should be extracted, the enzymes where deactivated by heating them according to the manual. Afterwards the samples where loaded on an agarose gel (see 3.2.1.6) for analysis or extraction.

3.2.1.5 Cloning of DNA constructs

Molecular cloning is the process to assemble and replicate recombinant DNA fragment by inserting them into a vector (plasmid in our case). By doing so it is not only possible to replicate and multiply a specific DNA fragment, but also to fuse it with other genes like a fluorescence tag or to combine it with a specific promoter. By inserting in a plasmid it is also possible to transfer the DNA fragment into a cell and let the genes be expressed. Cloning is therefore a crucial technique, especially for consecutive processes like transformation or transfection.

Protocol: The vector was cut (see 3.2.1.4) with a matching pair of restriction enzymes. Afterwards 2 µl of Calf Intestine Phosphatase was added and again incubated for 30 minutes at 37 °C. Afterwards it was loaded on a agarose gel (see 3.2.1.6) The vector fragment was extracted by cutting it out of the gel and extracting it using the QIAquick Gel Extraction Kit. The insert was either directly cut out with the same enzymes as the vector or was amplified by PCR (see 3.2.1.7) with primers with the respective cutting sites on the ends. The PCR product was loaded on an agarose gel and extracted the same way as the vector. The insert was then digested with the same restriction enzymes than the vector and purified by using the QIAquick Gel Extraction Kit.
Insert and Vector were added in a ratio of 1:5 (based on the size of the fragments) in an assay containing 1 µl T4 ligase and 1 µl buffer and filled up to 10 µl with ddH_2O. The samples were incubated at 16 °C over night. In the next day they where transformed to DH5α cells (see 3.2.1.2 and success was checked via restriction digestion and agarose gel.

3.2.1.6 Agarose gel electrophoresis

One of the most important techniques of analyzing DNA is the separation of its fragments via agarose gel electrophoresis. DNA fragments are negatively charged molecules that move along an electric field through the agarose gel, which acts as a molecular sieve - smaller fragments can pass it faster than lager ones. The fragments can be made visible by adding ethidium bromide to the gel which intercalates with the DNA and fluoresces under UV light.

Protocol: Agarose (1% (w/v) in 1xTBE) was heated in a microwave until it fully melted. The gel was then filled in an electrophoresis chamber and 0.5 µl ethidium bromide was mixed in. After the agarose cooled down the chamber was filled with 1xTBE buffer. The samples were loaded on the gel and a current of 80 mV was applied. Analysis was performed with a gel detection unit.

3.2.1.7 Polymerase chain reaction (PCR)

Developed in 1983 by Kary Mullis, the PCR developed to a standard technique for a broad variety of applications from gene amplification to genetic fingerprint analysis. The PCR relies on thermo cycling consisting of multiple repeats of the three phases denaturation, annealing and extension. During the denaturation phase, the DNA template is "‘melted"’ yielding single-stranded DNA molecules. The used DNA polymerase should be heat stable, because this step is usually

done at 94-98 °C. During the annealing phase, DNA primers can bind that are contemplary to the 3' ends of each of the sense and anti-sense strand of the DNA target. In the extension step a DNA polymerase is synthesizing a new DNA strand contemplary to the template. The temperature of this step is chosen by the polymerase's optimum activity temperature. Usually these steps are repeated 20-40 times. The DNA generated can itself be used as a template for replication, therefore the DNA template is exponentially amplified.

Protocol: Primers 5-9 (see 3.1.2.2) were used for PCR reactions. 1 µl of DNA template and 1 µl of both forward and reverse primer (10 µM) was put together with 10 µl of 5× polymerase buffer, 5 µl dNTP mix and 1 µl Q5 polymerase and filled up to a total volume of 50 µl with ddH_2O. The samples where put into a thermo cycler with the program from table 3.1.
Samples were transferred to an agarose gel (see 3.2.1.6 for analyzing and/or extraction.

Table 3.1: Thermo cycler program for PCR

Segment	Repeats	Temperature	Time
1	1	98 °C	30 s
2	35	98 °C 50 °C 72 °C	10 s 20 s 40 s
3	1	72 °C 4 °C	10 min hold

3.2.1.8 Site-directed Mutagenesis

The mutagenesis uses the principle of PCR to exchange single base pares. The amino acids sequence of the encoded protein can be modified that way. We used the ligation-during-amplification method where a plasmid is combined with a specific primer that carries the specific mutation. The mutation inside the primer is that way included in the plasmids that are created during the amplification. The unmodified template plasmid is digested in the following *DpnI* treatment, because this restriction enzyme is only cutting *dam* methylated DNA. Only one-stranded, modified plasmids remain. They are then transformed. Afterwards, a completed, modified plasmid carrying the desired mutation can be isolated.

Protocol: The samples contained 100 ng of template DNA and 100 ng of respective primer as well as 2.5 µl 10x Pfu buffer with $MgSO_4$, 0.5 µl Quick solution

(Stratagene), 5 µl 2 M dNTP mix and 1 µl Pfu polymerase at a total volume of 25 µl (filled up with ddH_2O).
The samples where put into a thermo cycler with the program from table 3.2. Afterwards, 1 µl of *DpnI* was added and the sample was incubated for 1 h at 37 °C. Then the cells where transformed (see 3.2.1.2). To see if the mutagenesis was successful the product had to be sequenced.

Table 3.2: Thermo cycler program for mutagenesis

Segment	Repeats	Temperature	Time
1	1	95 °C	1 min
2	30	95 °C 55 °C 65 °C	1 min 1 min 12 min
3	1	4 °C	hold

3.2.2 Protein Biochemistry

3.2.2.1 PC12 Lysates

For quantifying and analyzing the size of expresses proteins it is a classical approach to lysate cells and create an extract of all proteins. Afterward this extract can be analyzed by multiple ways for its composition. In our case we transiently transfected PC12 cells (see 3.2.3.5 with our gene of choice and then lysated the cells in a RIPA lysation buffer.

Protocol: The cells were cultured and transfected in 3.5 mm cell culture dishes and incubated for 3 more days after transfection. Then the medium was removed and the cells were washed two times in ice cold 1× PBS. After removing the PBS 90 µl lysation buffer was added and the cells were detached from the bottom of the dish with a cell scraper. Buffer and cells were transferred into an reaction tube and put on ice immediately. Then the tube with the lysate was incubated on a shaker for 30 minutes at 4 °C. Afterwards the lysates were centrifuged for 10 minutes at 10000 rpm and 4 °C. Supernatant was transferred into a new reaction tube. The lysate could be used immediately or shock frozen in liquid nitrogen and stored at -80 °C.

3.2.2.2 BCA Assay

The bicinchoninic acid assay is a biochemical assay for determining the total concentration of protein in a solution. The total protein concentration is exhibited by

a measurable color change of the samples from green to purple which is proportional to the total concentration of proteins. It primarily relies on two reactions. First, the peptide bonds in protein reduce Cu_2^+ ions from cupric sulfate in the working solution to Cu^+ where the amount of reduced Cu_2^+ is proportional to the amount of protein present in the solution. Next, two molecules of bicinchoninic acid chelate with each Cu^+ ion, forming a purple-colored product that strongly absorbs light at a wavelength of 562 nm. The bicinchoninic acid Cu^+ complex is influenced in protein samples by the presence of cysteine/cystine, tyrosine, and tryptophan side chains. At 37 °C peptide bonds assist in the formation of the reaction product. The total protein concentration can be quantified by measuring the absorption spectra and comparing with a standard consisting of solutions with known protein concentrations.

Protocol: The samples are diluted 1:5 in ddH_2O. BSA solutions with the concentration of 2000 µg/ml, 1500 µg/ml, 1000 µg/ml, 750 µg/ml, 500 µg/ml, 250 µg/ml and 125 µg/ml were used as a standard. Standard and samples were pipetted on a 96-well ELISA plate as triplets of 10 µl each. 200 µl of premixed working solution (according to the kit's manual) were added and then the samples were incubated for 30 minutes at 37°. Afterwards the samples were analyzed in an ELISA reader. The dilution was considered in the final concentration.

3.2.2.3 SDS-PAGE

By sodium dodecyl sulfate polyacrylamid gel electrophoresis (SDS-PAGE) proteins can be separated by their size. sodium dodecyl sulfate binds to proteins, giving them an overall negative charge. Then they move along an electric field through the polyacrylamid which acts as a molecular sieve. The "speed" of movement through the gel is indirectly proportional to the size of the proteins with big ones moving slower and small ones moving faster. For later analysis of the proteins afterwards the gel can be stained directly or the proteins can be transferred to a membrane via western blot.

Protocol: The gel consisted of two components, a separation gel in the lower part and a stacking gel in the upper part. The composition of the gels can be found in table 3.3. The separation gel was founded between two tightly connected glass plates and covered with isopropanol. After polymerization the isopropanol was removed and the stacking gel was founded in a second layer. After polymerisation the seal was removed and the gel inside the glass plates was inserted into the electrophoresis chamber that was then filled with buffer.

20% 5×Laemmli buffer was added to the samples and they were heated up to 95 °C for 10 minutes.
Then 5-20 µl of the samples (containing 20 µg of proteins) or 5 µl Protein ladder was transferred to the gel and a constant voltage of 100 V was applied for 90 minutes.

Table 3.3: Composition of SDS gels

	Separation gel 10%	Stacking gel 6%
Acrylamid/Bis	1 ml	200 µl
4× Lower Tris	750 µl	-
4× Upper Tris	-	250 µl
ddH_2O	1.25 ml	550 µl
10% APS	20 µl	5 µl
TEMED	3.5 µl	1 µl

3.2.2.4 Western Blot

Western blotting is a technique to transfer proteins form an polyacrylamid gel to a polyvinylidene fluoride membrane (PVDF) and make them accessible for immunostaining. By applying a constant electric field the proteins are wandering from the gel to the membrane where they are bound.

Protocol: In a grid a piece of felt and on top of it a piece of filter paper is applied and soaked with transfer buffer. After separating the glass plates the stacking gel is removed and the separation gel is then placed on the filter paper. The PVDF membrane is activated in methanol and then placed on the gel. All was covered then with another layer of filter paper and felt. It is important that all the components are soaked with transfer buffer and no air bubbles remain. The grid was closed and placed into the western blotting tank. A constant electric current pf 100 mA was applied over night.

3.2.2.5 ECL Immunodetection

Antibodies can be a useful tool to detect specific proteins, for example when they are bound on a PVDF membrane. The epitope of the primary antibody is specific for the protein that should be stained and a secondary antibody, linked to *horse radish peroxidase* (HRP) is binding to the primary antibody. HRP is catalyzing a chemoluminescent reaction of luminol. This reagent is added as part of an ECL

solution (enhanced chemoluminescene) and the light emitted by that reaction can be detected with a detection unit.

Protocol: The PVDF membrane is incubated in 15 ml of 5% (w/v) milk powder (solved in 1×TBS-Tween) for 1 hour on a seesaw to block remaining reactive groups. The membrane was then washed 3 times for 5 minutes in 1×TBS-Tween. Then it was incubated for 105 minutes in 5 ml primary antibody solution (Dilution 1:5000 in 5% milk powder in 1×TBS-Tween) on a seesaw. Afterwards it was again washed 3 times for 5 minutes in 1×TBS-Tween before the membrane was incubated in secondary antibody solution (Dilution 1:20000 in in 1×TBS-Tween) for 45 minutes on a seesaw. It was then washed 3 times for 5 minutes in 1×TBS-Tween again. 1 ml of ECL detection solution was put directly on the membrane and then it was detected in an ECL detection unit.

3.2.3 Cell Culture

Cultures were stored and incubated in an incubator at 37 °C and 10% CO_2. Media were stored at 4 °C and warmed up to 37 °C before use in a water bath.

3.2.3.1 Culture of PC12 cells

Phaeochromocytoma cells (PC12) were first isolated from a rat's adrenal gland tumor. Cells from the adrenal gland have their origin in the neural crest and are therefore related to neuronal cells. One essential part of this heritage is the fact that when treated with Nerve Growth Factor, they show a neuron-like development and form axon-like neurites. This makes PC12 cells to a easy-to-handle model system for neuronal cells.

Protocol: All work was done under S1 conditions. PC12 cells are cultured in a 10 cm cell culture dish in 10 ml DMEM all inclusive medium. Every 3-4 days the cells reached confluency. Then they had to be splitted by removing the old medium, dissolving and resuspending the cells from the bottom of the dish in 5 ml DMEM all inclusive. 1 ml was kept and transfered to a new dish and filled up to 10 ml with DMEM all inclusive. The rest was either discarded or kept as a backup and for plating out cells.

3.2.3.2 Culture of HEK293FT cells

The **H**uman **E**mbryonic **K**idney 293FT cell line is derived from human embryonal kidney cells transformed with sheared adenovirus 5 DNA and the SV40 large T antigen to generate high-titer lenti virus. HEK 293 cells are very easy to grow and transfect very readily.

Protocol: All work was done under S2 conditions. HEK293FT cells are cultured in a 10 cm cell culture dish in 10 ml DMEM complete medium and 100 µl G418. Every 3-4 days the cells reached confluency. Then they had to be split by removing the old medium and dissolving them by adding 500 µl trypsine and letting them rest for some minutes. The cells were then resuspended in 9.5 ml DMEM complete. 1 ml of resuspended cells were then transferred to a fresh 10 cm culture dish, filled up to 10 ml and 100 µl G418 was added.

3.2.3.3 Cell counting

To determine the number of plated cells, they were counted using a Neubauer chamber.

Protocol: The cells were resuspended in 5 µl DMEM all incl. 10 µl of cell suspension were mixed with 10 µl tryphane blue and 10 µl of this mixture were loaded on the Neubauer counting chamber. 4 squares were counted and the mean was calculated and multiplied by two (due to the dilution with tryphane blue). This result multiplied by 10^4 was the total number of cells per ml in the suspension.

3.2.3.4 Covering of live cell dishes

Covering dishes with collagen or laminine provided a surface on which plated cells could attach.

Protocol: All work was done under S1 conditions. Glass bottom dishes were covered with 750 µl poly-l-lysine solution and incubated over night. On the next day they were washed 2 times with ddH_2O for 1 hour each.
For PC12 cells, the dishes were covered with 750 µl collagen solution for 45 minutes. For primary culture neurons, the dishes were covered with 750 µl laminine solution for 6 hours. In both cases the dishes were washed 2 times with 1×PBS afterwards. The cells were plated directly after the last coating step.

3.2.3.5 Transient Transfection of PC-12 cells

Liposome-transmitted transient transfection is a technique for temporary insertion of a plasmid into an eucaryotic cell. The used transfection reagent is covering the plasmid and giving it a hydrophilic "cover" so that it can pass the cell membrane and get into the cell. It is a mild yet efficient method to transport a specific plasmid and therefore a desired gene into the target cells and to let it express the respective encoded gene.

Protocol: All work was done under S1 conditions. On the previous day 10^5 cells from a 10 mm cell culture dish were plated on a PLL and collagen coated glass bottom dish and 1.5 ml DMEM all inclusive was added. 80 µl OPTIMEM were provided in a polystyrene tube. 4 µl Lipofectamin™2000 were added for 5 minutes at room temperature. 80 µl were provided in a reaction tube and 2.5 µg DNA was added. Then the mixture was transferred into the polystyrene tube mixed throughoutly and incubated for 25 minutes at room temperature. Meanwhile the plated cells were washed with OPTIMEM and then 800 µl OPTIMEM was put in the cells. After the incubation time, 800 µl OPTIMEM was added to the mixture in the polystyrene tube and the whole mixture was transferred to the dish drop wise. After 5 hours of incubation at 37 °C 800 µl DMEM all inclusive was added to the culture dish. On the next day, the medium was removed and 1.5 ml DMEM all inclusive was put into the dish.

3.2.3.6 Transient transfection of HEK293FT cells

For the generation of replication deficit lenti viruses, a system of three plasmids is used: On of them carrying the gene of interest and two helper plasmids. Therefore a triple transfection is used for that. Once all three plasmids have entered the target cell, the combination of all three leads to synthesis of lenti viruses capable of stably inserting the gene of interest into the infected cell.

Protocol: All work was done under S2 conditions. 23.6 µl TransIT 293 and 1.18 µl OPTIMEM were put together into a polystyrene tube and incubated for 10 minutes at room temperature. Then 5 µg L22 plasmid DNA, 3.75 µg L3 helper plasmid and 1.5 µg L4 helper plasmid (see 3.1.2.1) was added and the mixture was incubated for another 20 minutes at room temperature. The old medium was removed from the 10 cm culture dish containing the HEK293FT cells and 10 ml of fresh DMEM complete medium was added. Then the mix from the polystyrene

tube was added to the dish. The cells where then incubated for 72 hours at 37 °C and 5% CO_2. Afterwards the virions could be harvested.

3.2.3.7 Harvesting and concentration of lenti virus

By performing a triple transient transfection with a L22 lenti viral vector bearing the gene of interest and two helper plasmids we are able to transform HEK293FT cells into a production unit for replication-deficient, self-inactivating lenti viruses capable of infecting the gene of interest directly into the genome of the target cells. The HEK cells release these virions into the surrounding medium, where they can be harvested.

Protocols: All work was done under S2 conditions. The supernatant from the 10 cm culture dish was collected using a 20 ml syringe and then filtered and transferred into an ultraclear centrifuge tube using a 0.45 µm syringe filter. The tubes were centrifuged for 90 minutes at 115000 ×*g* (25,000 rpm) and 4 °C using a Sorvall Discovery 90SE ultracentrifuge with a Surespin 630 rotor. After centrifugation, the supernatant was carefully decanted into liquid S2 waste. The pellet was resuspended in 100 µl MEM and left standing at 4 °C overnight. Following the incubation, the virus was aliquoted and shock frozen in liquid nitrogen. The aliquots were for single use and has been stored at -80 °C. Viruses were characterized and transfection efficiency was determined by infection of PC12 cells and determining the ratio of infected to total cell number. The mice were bred for three days. 16 days after breeding (calculated from second breeding day), the mice were sacrificed by cervical dislocation. The abdominal wall was opened and the uterus containing the embryos was removed and placed on a EtOH saturated tissue. The embryos where extracted from the uterus and the amniotic sac and transferred to a sterile HBBS-filled /unit10cm cell culture dish and resting on a cool pack. The head was dislocated and the linnings of the brain were removed with forcepses. The dissected cortexes of the brain were separated and transferred to a reaction tube containing 500 µl MEM and put on ice.

3.2.3.8 Preparation of primary culture neurons

From now on all work was performed under S2 conditions. The cells were dissociated mechanically by trituating through a Pasteur pipette. The pipette was flame treated before trituation to avoid sharp edges on the opening. The samples were put on ice for some minutes to let the remnants of the linings of the brain sed-

iment. The supernatant was transferred into a 15 ml tube and was centrifuged at 700 rpm for 15 minutes at 4 °C. The supernatant was removed and the pellet was resuspended in 500 µl NB/B27. Afterwards the cells were counted and 5×10^4 cells were plated on a laminine coated glass-bottom dish (see 3.2.3.4) and filled up with 1.5 ml NB/B27.

3.2.3.9 Infection of cells with lenti virus

Transfection is not working for all model organisms. An alternative method of inserting genes into cells *in vivo* viruses can be used as a vector. Especially lenti viral vectors have the great benefit of stably inserting genes of interest into the genome of model cells.

Protocol: 5-10 µl of virus aliquot (dependant of infection efficiency) was added to the glass bottom dish containing plated PC12 or primary culture cells. Imaging was performed 6 days after infection.

3.2.3.10 NGF treatment

By treating PC12 cells with *Nerve Growth Factor* (NGF), differentiation can be induced similar to neuronal cells: The cells start to develop processes or neurites that show similar characteristics to neural axons. By that PC12 cells can be used as a neuron like cell model that is easy to handle.

Protocol: On the second and fourth day after transfection the cells were treated with NGF. The old medium was removed and 1.5 ml DMEM 1% without phenole red was added. Also 15 µl NGF was added.

3.2.4 Live Cell Imaging

3.2.4.1 Aquisition

All imaging was performed with the confocal laser scanning microscope Nikon Eclipse TE2000-U with confocal C1 scan and detection unit. The microscope was equipped with a 405 nm Blue-Diod laser, a 488 nm argon laser and a 543 nm helium/neon laser. The microscope stage is equipped with an incubation chamber and a CO_2 enrichment chamber made by Solent Scientific Ltd. to ensure that the cells are kept at 37 °C and 10% CO_2. A 60× oil immersion objective (Numerical aperture 1.40) by Nikon was used for recording.

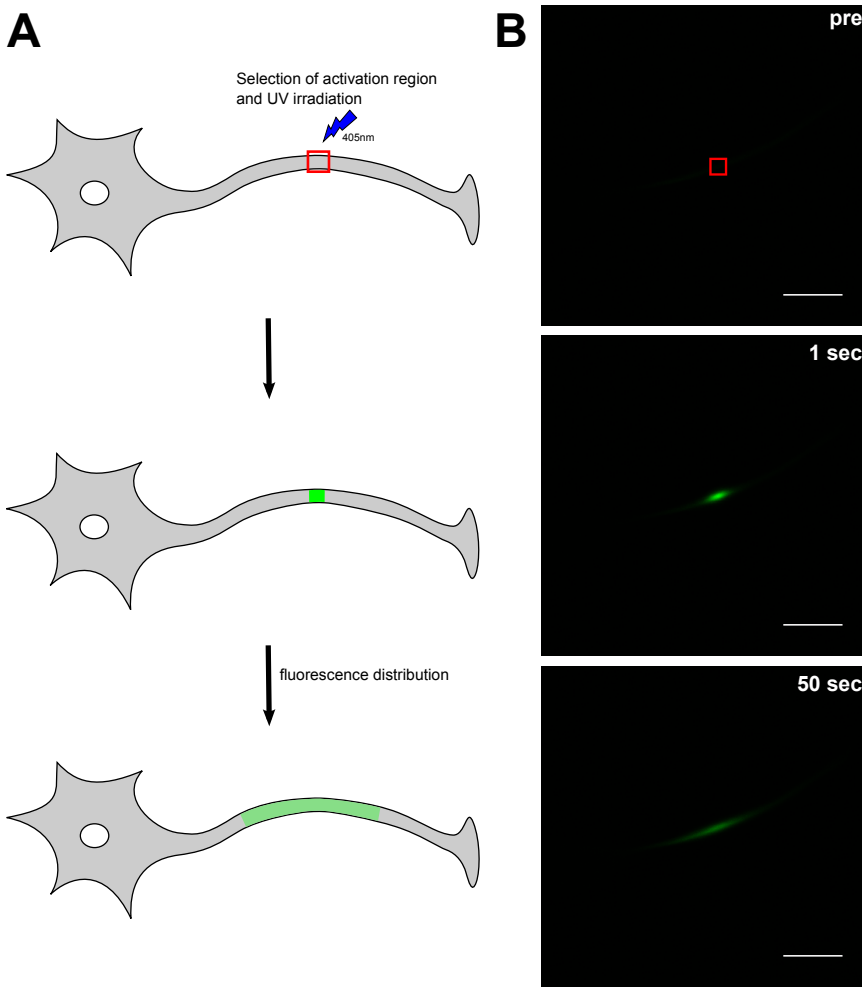

Figure 3.1: **Schematic (A) and showcase (B) representation of photoactivation approach.** The region of activation is chosen and the PAGFP is photoconverted by UV irradiation at 408 nm. The distribution of fluorescence can be observed over time.Scale bar 10 µm

PAGFP-positive cells were detectable by week green fluorescence. For the excitation a 488 nm laser was used. Only cells were chosen which had straight processes minimum the size of the cells diameter. The activation region of the program was set on the middle or the tip of the process. The detector gain was then reduced so that the cell was not longer visible. Then the photoactivation macro was started; the PAGFP was photoconverted with a 408 nm laser for 1 second and after activation a picture was recorded every second for a duration of 112 seconds (for microscope settings see also table 3.5).

3.2.4.2 Evaluation

The recorded data sets consisted of 113 frames each. The first frame was recorded before photo conversion (from now on called "photoactivation") and

Table 3.5: Microscope settings

Settings	
Pixel dwell	4.08 µs
Field of view	100 µm
resolution	256 × 256 pixel
Number of frames	112
Frame delay	1 s

is considered as the background frame. The evaluation was performed using Fiji, an image processing package of ImageJ. The activated region was selected with a rectangle and the length of the rectangle was noted (see Figure 3.2 A). Only regions with approximately the same length were chosen for further evaluation. The sum of the gray values of the pixels inside the selected area (called "Raw Integrated Density") is then calculated by Fiji for every frame (see Figure 3.2 B). These values represent the "brightness" of the fluorescence in the activated region. To subtract the background of the picture, the first value is subtracted from every other value in the set. Afterward the values were normalized to the first value after photoactivation, which is considered the one with the most fluorescence. All values are divided by the value of the first frame after photoactivation (see Figure 3.2 C). The results show the remaining fluorescence in the activation region relative to the first frame after photo activation. These values were plotted as a curve and resemble the fluorescence decay after photoactivation in the activated region, which we used as a marker for protein mobility.
Statistical analysis among experimental groups was performed using one-way analysis of variance (ANOVA). For analysis of FDAP curves the values at time point 10 s and 50 s were used, the P-value was $P<0.05$.

3.2.4.3 Modeling and Fitting

For modeling the parameters of tau/microtubule interaction we determined a model of a tube where a fraction of unbound proteins (C) and binding partners (B) are in steady state with a fraction of bound proteins (S) as can be seen in equation 3.1.

$$C + B \underset{k_{off}}{\overset{k_{on}}{\rightleftharpoons}} S \tag{3.1}$$

For C and S the concentrations $c(\vec{r}, t)$ and $s(\vec{r}, t)$ are determined mathematically. $c(\vec{r}, t)$ and $s(\vec{r}, t)$ are then summed up and averaged over the whole activation area (see figure 3.2). By doing so a theoretical curve could be calculated repre-

senting the parameters of tau interaction.
Afterwards the evaluated data were fitted to the curve according to the method of least squares. A script was written to compare the evaluated data with the theoretical curve and determines the values for k^*_{on} and k_{off} for which the sum of squared residuals for the parameters was minimal. The value k^*_{on} stands for the *association rate* which describes how many tau molecules attach to the microtubule surface per second - it is an *apparent* association rate, which is defined as product of *kon* and the fraction of free binding partners B_{eq} (see also equation 3.3 and 3.4. The value k_{off} is the *dissociation rate* describing the number of tau molecules detaching from the microtubule surface per second.
From this data, we were able to derive the fraction of bound tubulin. We define the equilibrium constant K_{eq} of equation 3.1 by the equations 3.2 and 3.3. From these two definitions we can derive that the ratio of apparent association constant to dissociation constant is equal to the ratio of bound to unbound fraction of protein (equation 3.5). By assuming that the total concentration of protein c_{total} is the sum of the concentrations of bound and unbound protein, we can calculate the relative fraction of unbound protein $\frac{C_{eq}}{c_{total}}$ by combining equations 3.6 and 3.7. $\frac{C_{eq}}{c_{total}}$ is a relative value, we do not need to know the actual concentration of proteins.

$$K_{eq} = \frac{k_{on}}{k_{off}} \tag{3.2}$$

$$K_{eq} = \frac{S_{eq}}{C_{eq} \cdot B_{eq}} \tag{3.3}$$

$$k^*_{on} = k_{on} \cdot B_{eq} \tag{3.4}$$

$$\frac{k^*_{on}}{k_{off}} = \frac{S_{eq}}{C_{eq}} \Longrightarrow S_{eq} = \frac{k^*_{on}}{k_{off}} \cdot C_{eq} \tag{3.5}$$

$$c_{total} = C_{eq} + S_{eq} \tag{3.6}$$

$$\Rightarrow \frac{C_{eq}}{c_{total}} = \frac{1}{1 + k^*_{on}/k_{off}} \tag{3.7}$$

This approach is based on unpublished work of Maxim Igaev.

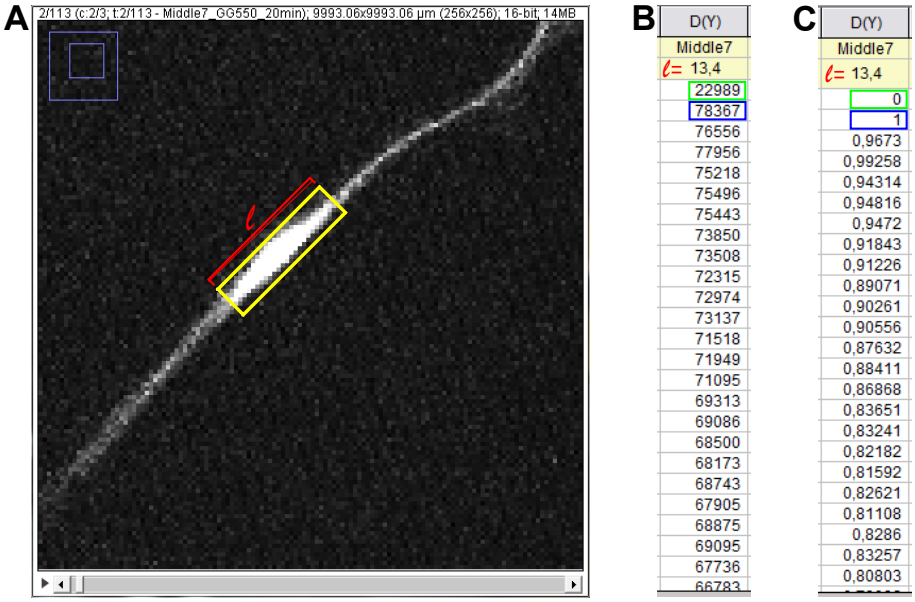

Figure 3.2: **Evaluation of FDAP acquisitions.** **A** The region of activation is marked (yellow box) and its length is determined (*l*). **B** Then the raw integrated intensity is measured for all 113 frames. **C** The background intensity(green box) is subtracted from all values. Then all values are normalized by dividing through the value of the first frame after photo conversion (blue box).

4 Results

4.1 Characterization of Tau Fragments

4.1.1 Functional Organization of the Interaction of Tau with Microtubules in PC12 cells

Binding of tau to microtubules requires the repeat domain in the c-terminal half of tau protein that consists of 3-4 highly homologous repeats [50]. We want to know whether the number or the specific position of the repeats has a direct influence of tau mobility in neuronal cells *in vivo*. We also want to address the effect that the number of repeats has on biophysical constants of tau-microtubule-interaction in living cells. For this we created tau fragments by replacing amino acids glutamine 276, glutamine 307, glutamate 338 or lysine 369 with stop codons via site-directed mutagenesis (see green letters in Figure 2.3). The re-

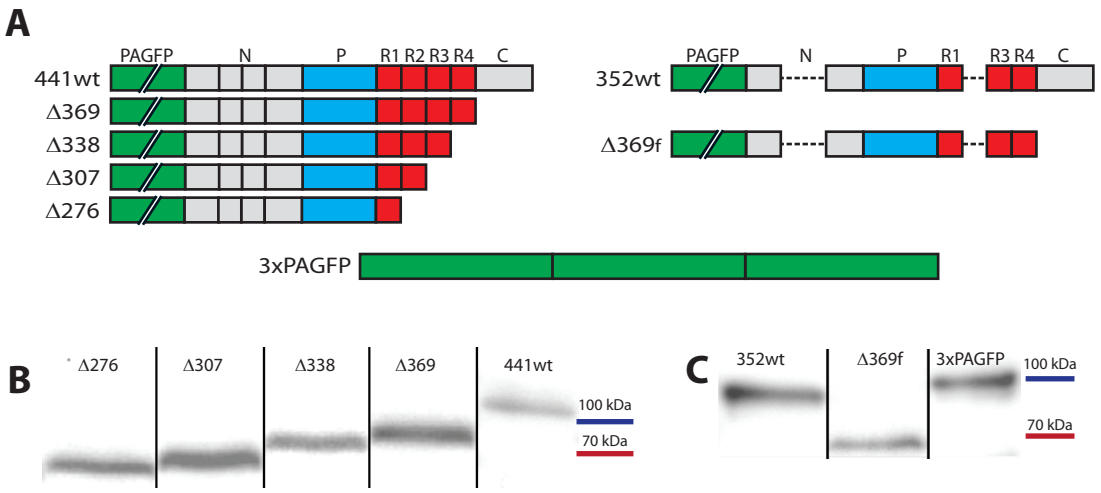

Figure 4.1: **Characterization of tau truncation fragments by western blot.** Schematic representation of PAGFP-tagged tau truncation products and a control construct 3xPAGFP (**A**). Western blots show the expression of tau constructs in PC12 cells for fragments derived form htau441wt (**B**) and htau352wt (**C**). Immunostaining was performed with chickenαGFP antibody

sults are four tau fragment constructs which differ in their numbers of repeats in their repeat domains and that all lack the carboxy-terminal part (see Figure 4.1). All fragments were tagged with a PAGFP on their amino terminal end to perform **f**luorescence **d**ecay **a**fter **p**hotoactivation (FDAP) experiments. The sequence was embedded in a pCMV vector so that they could easily be transfected into PC12 cells for further investigation. To have a control for a non-interacting protein, we used 3×PAGFP which consists of three copies of PAGFP linked together to one molecule, which has approximately the size of PAGFP-htau441wt. We also used a PAGFP-tagged tau 352wt, which lacks exon two and three as well as repeat two. To see if repeat two has a specific function, we also created a fragment of tau352wt which has three repeats like Δ338 and also lacks the c-terminus. We used the same primer as for Δ369 and consequently named the fragment Δ369f (f stands for "fetal"). The fragment plasmids were transiently transfected into PC12 cells and four days of NGF-treatment was performed to differentiate the cells and animate them to develop processes. We looked at the middle of the process because here it is very flat and narrow compared to the cell body. Due to this shape it can be treated as a pseudo two dimensional system where proteins can diffuse only in two directions.

We performed FDAP experiments with full length tau (tau441wt) and its fragments and compared the fluorescence decay of it with non-interacting control protein 3×PAGFP. We analyzed the relative intensity of fluorescence in the region of activation and compared it to the first frame after photoactivation. The control construct showed a very rapid fluorescence decay while the FDAP of full length tau was significantly slower (Figure 4.2 A, table 4.1). With decreasing number of repeats the the FDAP was increasing for fragments constructed from tau441wt. For Δ369 the fluorescence deday is already significantly lower than for tau441wt. So a truncation after repeat 4 already has an influence on tau mobility. Deletion of repeat 4 results also in a decreased FDAP although the difference between Δ369 and Δ338 is not significant. Fragments that only had one or two repeats left showed the same mobility as the 3×PAGFP control; there is no significant difference between the FDAP of Δ307, Δ276 and 3×PAGFP. Since this control protein does not interact with other proteins at all we reason that these two fragments don’t interact with microtubules, so a minimum of two repeats is needed for tau to properly interact with microtubules. The FDAP of tau352wt (Figure 4.2 D) is similar to tau441wt; It shows no significant difference. FDAP for Δ369f is significantly lower than for tau352wt - this observation is analog to tau441wt and Δ369. Both Δ338 and Δ369f, which both have three repeats left, show a similar FDAP, although Δ369f is 89 amino acids smaller than Δ338 because it lacks exon two and three. The difference between the two curves is not significant.

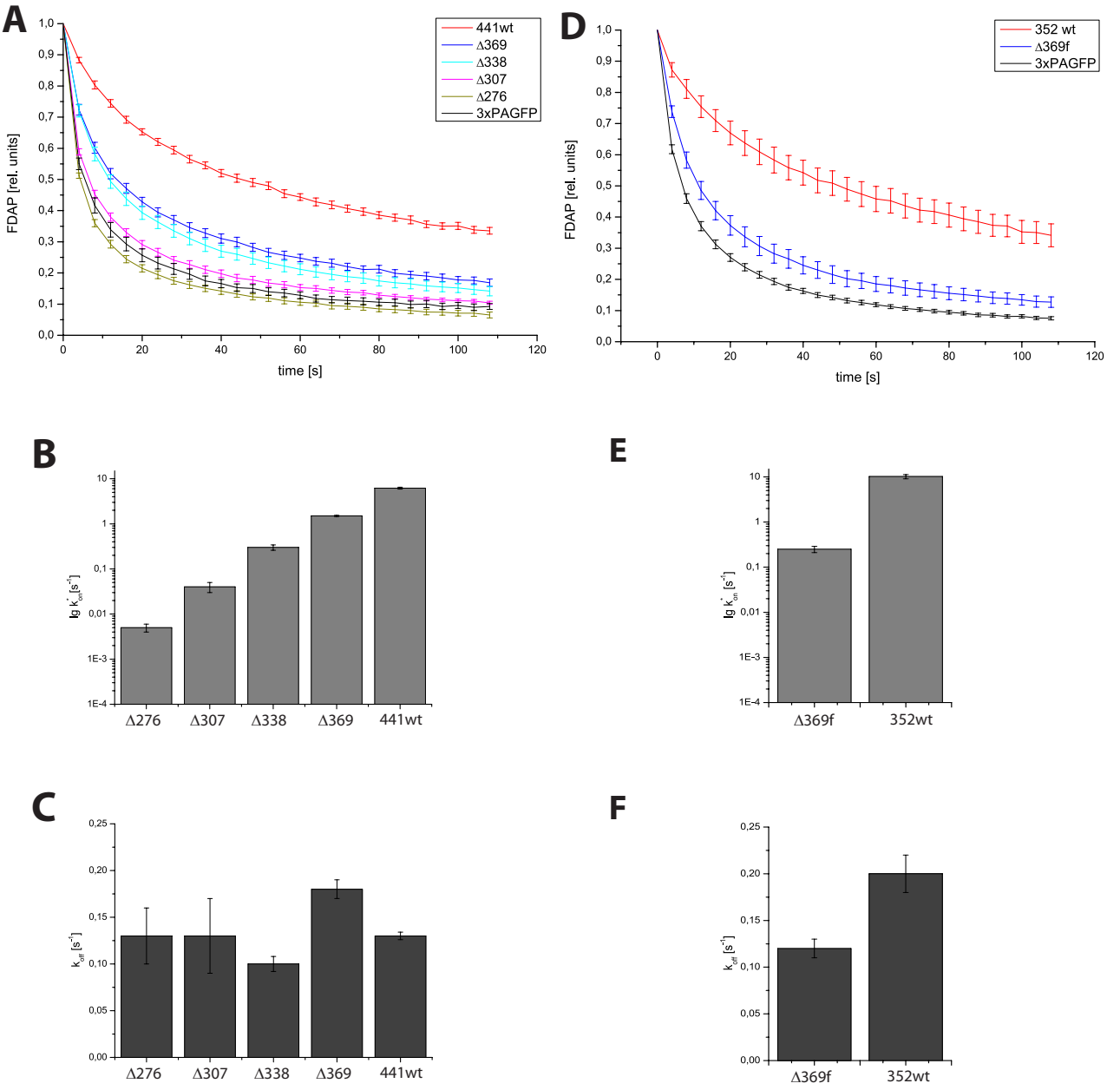

Figure 4.2: **Fluorescence decay after photo activation (*FDAP*) and association and dissociation rates of tau and its fragments in the middle of the process**. The FDAP of tau441wt and its fragments increases with decreasing number of repeats. (**A**). The association rate k^*_{on} (**B**, displayed as decadic logarithm) is decreasing, the dissociation rate k_{off} (**C**) stays nearly the same. The FDAP of tau352wt is similar than for tau441wt, its fragment Δ369f has an increased FDAP that matches to the correspondent fragment of tau441wt (Δ338). n = 13-15 (**D**). The association rate k^*_{on} of tau352wt is higher than for tau441wt (**E**, displayed as decadic logarithm). Unlike for the 441-fragments the dissociation rate k_{off} for Δ369f is lower than for the wild type (**F**). A+D show the mean value ± standard error, n = 14-19. k^*_{on} and k_{off} are calculated values including an error estimation.

Table 4.1: **Statistical analysis of FDAP curves of tau and its fragments in the middle of the process.** The significance was calculated using One way ANOVA (P<0.05) for FDAP values at 10 and 50 seconds. + indicates that the curves are significantly different in both values, - means no significant difference. The respective curves can be seen in figure 4.2 A+D.

	441wt	Δ369	Δ338	Δ307	Δ276	352wt	Δ369f	3×PAGFP
441wt		+	+	+	+	-	+	+
Δ369	+		-	+	+	+	-	+
Δ338	+	-		+	+	+	-	+
Δ307	+	+	+		-	+	+	-
Δ276	+	+	+	-		+	+	-
352wt	-	+	+	+	+		+	+
Δ369f	+	-	-	+	+	+		+

The association rate of tau441wt and its fragments are decreasing with decreasing numbers of repeats (Figure 4.2 B) from $6.2\,s^{-1}$ down to $0.3\,s^{-1}$ for Δ338 (which, according to figure 4.2 A is the last fragment that shows interaction with microtubules) and down to $0.04\,s^{-1}$ for Δ307 and $0.005\,s^{-1}$ for Δ276 which show no interaction at all. The dissociation rate for tau441wt, Δ307 and Δ276 are the same ($0.13\,s^{-1}$), while the rate is slighly increased for Δ369 ($0.18\,s^{-1}$) and slightly decreased for Δ338 ($0.10\,s^{-1}$). This leads to the conclusion that the reduction of the total number of repeats of tau441wt mainly leads to a decreased ability of association with microtubules, while the dissociation is lowly affected. The association and dissociation rate of tau352wt (Figure 4.2 E+F) are both higher than the rates of tau441wt, so the fetal form attaches and detaches more often when it comes to microtubule interaction. The fetal tau fragment Δ369f shows a slightly lower association rate ($0.25\,s^{-1}$) than its comparable full length fragment Δ338, its dissociation rate ($0.12\,s^{-1}$) on the other hand is similar to the rate of 441wt but slightly higher than for Δ338.
From the association and dissociation rates, we were able to derive the fraction

Table 4.2: **Fraction of microtubule-bound tau fragments**. With decreasing number of repeats, less tau protein is bound to microtubules. Standard errors are shown below each value. n = number of cells. D = diffusion coefficient

	441wt	Δ369	Δ338	Δ307	Δ276	352wt	Δ369f
Bound fraction	98%	89%	75%	23%	4%	98%	67%
Standard error	0.15	0.15	0.28	0.16	0.02	0.42	0.28
n	15	16	19	14	14	13	15
D in m^2/s	14.4	15.0	15.3	15.6	15.9	14.9	15.3

of microtubule-bound tau fragments (for the calculation see 3.2.4.3 on page 33). Table 4.2 shows that for both wild types (tau441+352) the fraction of bound tau is 98%, which matches with the observation that 352wt is dissociation and association with a higher rate but still show the same mobility when looking at the FDAP. With decreasing number of repeats also the fraction of microtubule-bound tau is decreasing for both full length and fetal tau fragments.
We were also able to calculate the diffusion coefficient of all tau fragments according to the Stokes-Einstein equation. This coefficient describes the movement of tau and its fragments by diffusion in a system without interaction hindering it. The differences between the fragments are result of the different sizes of the fragments and therefore a different hydrodynamic radiuses.
We excluded Δ276 from further investigations, because this fragments shows no microtubule interaction at all and continued with the other fragments with Δ307 as our no-more-interaction control.
Growth cones are specialized structures that are in a constant state of reorganization. Microtubules transiently enter the peripheral region via dynamic instability and are stabilized to promote process growth and growth cone movement. So the tip of a process can be seen as a very dynamic structure compared to the middle. address tau mobility in the tip, performed FDAP experiments by photoactivation in the tip of the processes (Figure 4.3 A). Due to the shape, the fluorescence could distribute only into one direction of the process (Figure 4.3 B), which is also reflected in the FDAP curves (Figure 4.3 C) by their more shallow slope. We found that also in the tip of the process truncation of tau and with it reduction of the number of repeats leads to an increase of FDAP. However the differences between the curves are much smaller than in the middle of the processes. Except for the wild types, the the FDAP curves of the tau fragments are not significantly different from the curve of 3×PAGFP.

Table 4.3: **Statistical analysis of FDAP at the tip of the process.** Significance was calculated using One way ANOVA (P<0.05) for FDAP values at 10 and 50 seconds. + indicates that the curves are significantly different in both values, - means no significant difference. The respective curves can be seen in figure 4.3 C+D.

	441wt	Δ369	Δ338	Δ307	352wt	Δ369f	3×PAGFP
441wt		-	+	+	-	-	+
Δ369	-		-	+	-	-	-
Δ338	+	-		-	-	-	-
Δ307	+	+	-		+	-	-
352wt	-	-	-	+		-	+
Δ369f	-	-	-	-	-		-

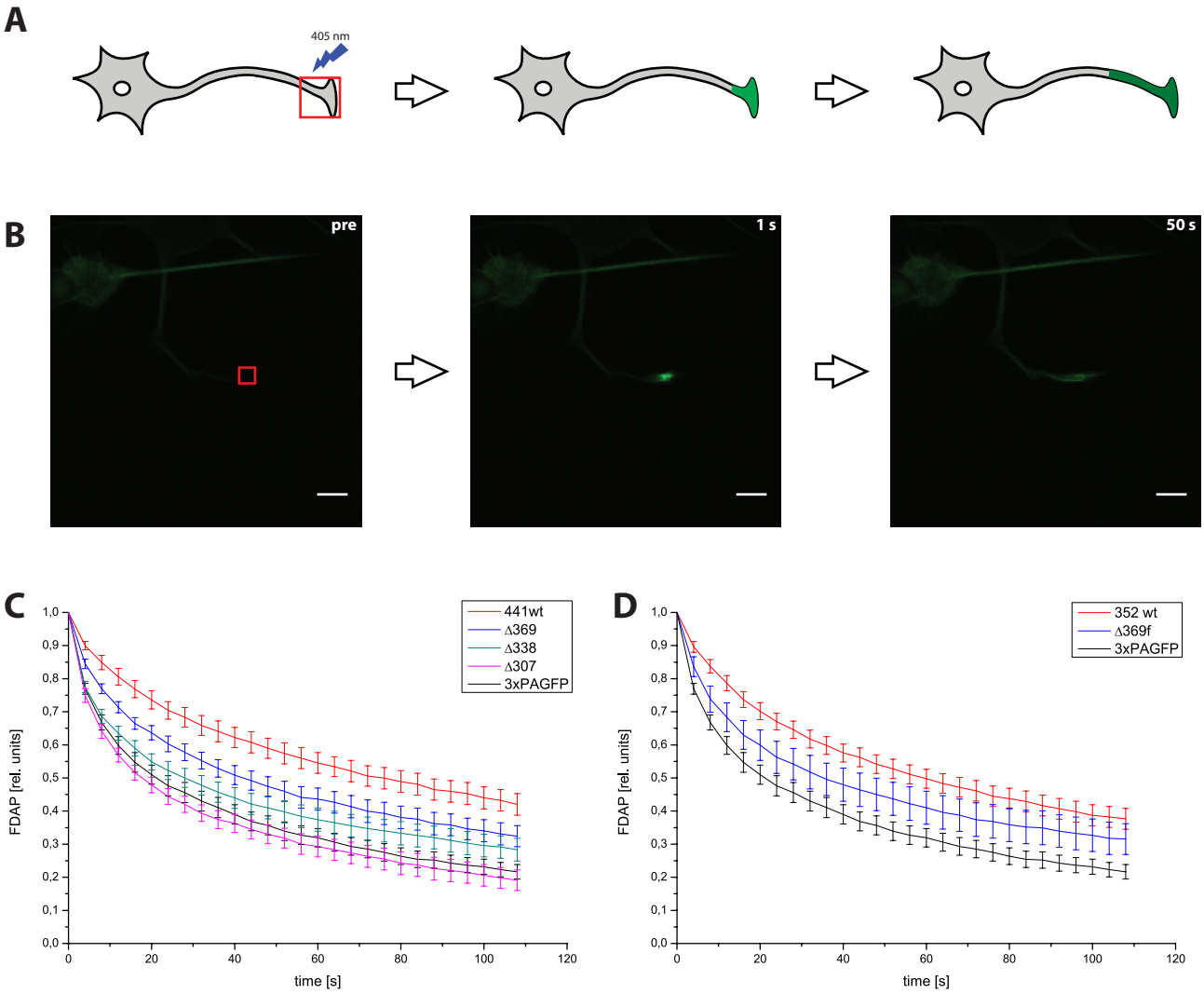

Figure 4.3: **FDAP at the tip of the process**. Schematic representation of photo activation and fluorescence distribution at the tip of the process (**A**) and example (**B**) with activation area (red box) before (pre) and 1 and 50 seconds after photo activation. Scale bar, 10 µm. FDAP at the tip of the process for htau441wt and its fragments (**C**) is increasing with decreasing number of repeats. Despite the differences in shape, the FDAP for tau441wt is almost similar in middle and tip, and lower for the fragments. The same can be observed for htau352wt and its fragment (**D**). C+D show the mean value ± standard error, n = 11-17.

To see if PC12 cells are a valid model system for the processes in neuronal cells we compared the interaction of PAGFP-htau441wt with the interaction in primary culture neurons. We used a lenti viral vector to express PAGFP-tagged human tau, analyzed the dynamics in axons and dendrites separately and compared it with the results we previously received. In figure 4.4 we can see no significant difference between the FDAP of the different cell systems. This is congruent to former work in this group [29], where it could be shown that the interaction of tau 352wt and the membrane associated protein Annexin A2 in PC12 cells was comparable with the interactions in primary culture neurons. When we look at the association rate though, we see that k^*_{on} is higher for PC12 cells than for primary neurons. Also the k_{off}-rate for axons is slightly lower than for PC12 cells, while it is higher for dendrites, but with a very huge error estimation. The difference in the apparent association rate indicates that tau-microtubule interaction is lower in primary culture neurons. For this we have to keep in mind that the expression levels are different: The CMV promoter that was used for transient transfection in PC12 cells has a higher expression rate than the CaM kinase II promoter we used in primary culture neurons. Another finding of this experiment is that there is no significant difference in FDAP between the compartments. So although tau is primarily found in the axon of neurons [8, 12], mobility of tau does not depend on the compartment, as it can be seen here that there is no significant difference between FDAP in axon and dendrite. Also on level of the association rate there is no difference between axons and dendrites. The dissociation rate is higher in dendrites, but again we have to keep in mind the high error estimation.

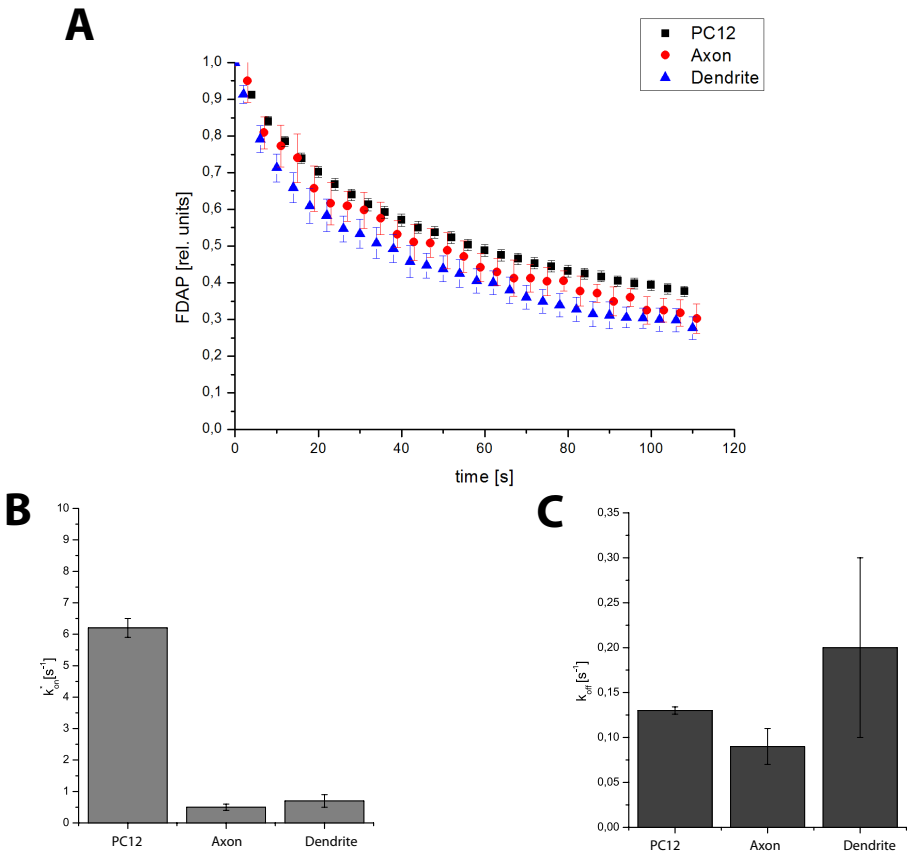

Figure 4.4: **Comparison of FDAP in PC12 cells and primary culture neurons.** Axons and dendrites were analyzed separately. No significant difference can be seen between the FDAP of the different model systems or between compartments. Mean values ± standard error, n = 15 (PC12) / 6 (Axon) / 8 (Dendrites). (**A**). The association rate k^*_{off} for tau441wt is higher than in primary neurons. However there is no difference between k^*_{off} in axons and dendrites (*B*). The dissociation rate is a bit higher in PC12 cells than in axons and it is much higher for dendrites, although the error estimation is very high (**B**).

4.1.2 Interaction of Tau and its Fragments on stabilized and destabilized Microtubules

For tau-microtubule interaction not only tau is relevant, but also the state that microtubules are in. The dynamic instability of microtubules can be affected by multiple factors, and possibly the interaction with tau is one of them, too. We examined the influence of microtubule stability have on tau mobility and microtubule interaction by using destabilizing and stabilizing agents.

Colchicine is a toxic alkaloid found in *Colchicum autumnale*. It is used in cancer treatment as a mitosis inhibitor where it prohibits the formation of a spindle apparatus. It binds to a Colchicine-binding site located on β-tubulin. A portion of this site is constituted by residues 1-46 and 214-241; these Colchicine-binding regions are also involved with GTP binding and, thus, represent active regulatory domains of β-tubulin [66]. It is also proposed that Pro268 and Ala248 are crucial for the specificity of Colchicine for animal tubulin [5]. Binding of Colchicine to tubulin inhibits tubulin polymerization in animal cells. Treated with Colchicine these cells consequently show more free tubulin dimers that cannot bind anymore to microtubules; the balance between bound and unbound tubulin is distracted and so is microtubule stability.

We transiently transfected PC12 cells with both wild type tau isoforms and the microtubule-interacting fragments Δ369 and Δ338. We also used Δ307 and 3×PAGFP as a control. After four days of NGF treatment we treated the transfected cells for 30 minutes with 10 μM Colchicine (dissolved in ddH_2O) or ddH_2O as a carrier control. Imaging was performed for maximum 1 hour after treatment to exclude any effects from long-time incubation, so the maximal duration the cells where exposed to Colchicine was 90 minutes.

As expected we saw no differences in FDAP for 3×PAGFP and for Δ307 (Figure 4.5 A) hence the fact that both of them are known not to bind to microtubules (see 4.1.1 on page 36). Also for Δ369 and for tau352wt we could only observe a very low effect and an only slightly increased FDAP that is not significantly different from the ddH_2O control. We however observed a significant difference between Colchicine treatment and carrier control for cells transiently transfected with tau441wt ($P<0.05$). We saw an increased FDAP for Δ338 transfected cells treated with Colchicine compared to the carrier control; the fluorescence decay is higher in the first half and is approximating to the fluorescence decay of the carrier decay in the second half. Statistical analysis could not proof significance for this difference.

The association rate (Figure 4.5 B) for both wt tau isoforms is slightly decreased for Colchicine treated cells compared to carrier control, an effect that can be ex-

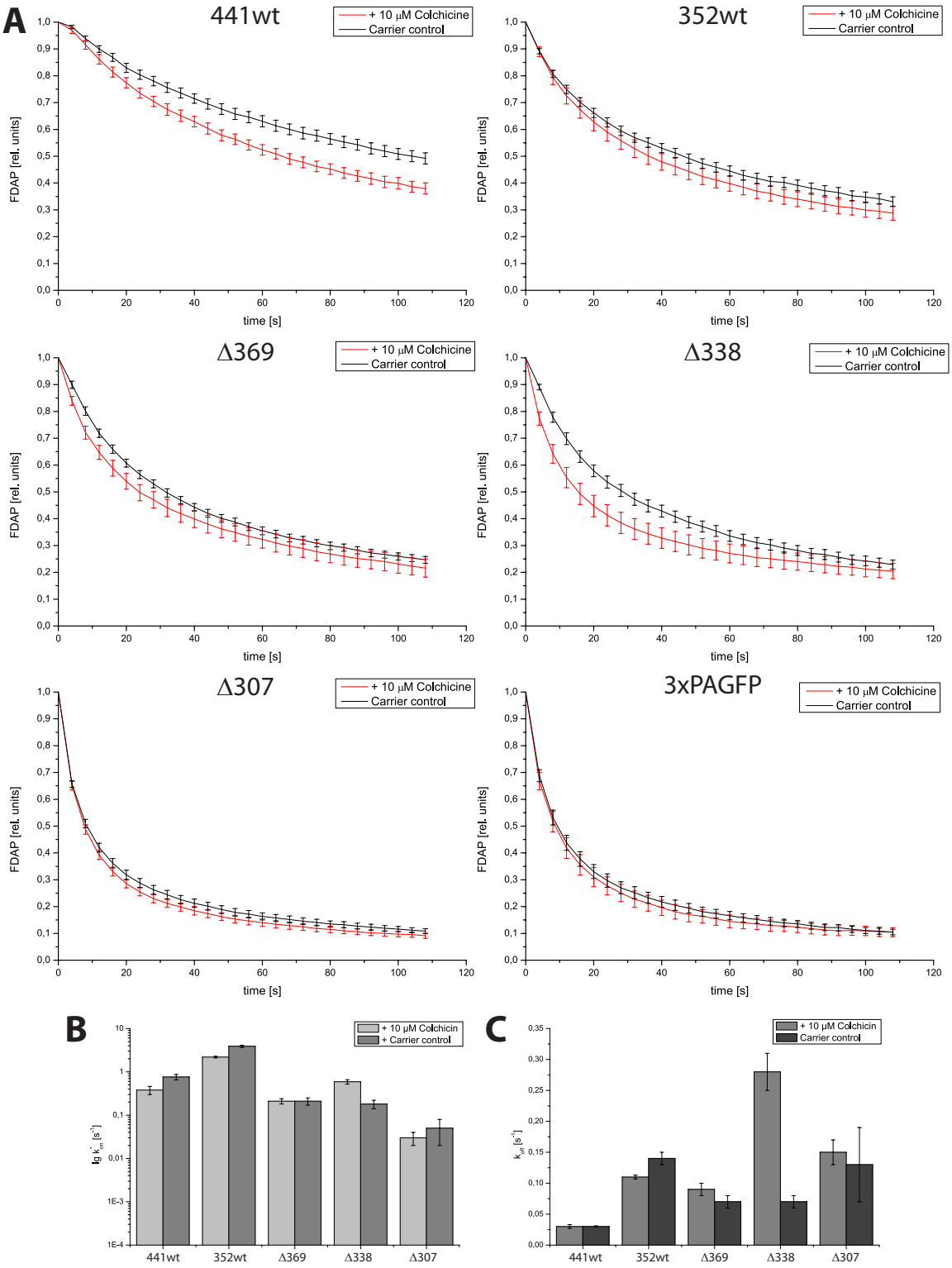

Figure 4.5: **FDAP and association and dissociation rates of tau and its fragments in the middle of the process with and without Colchicine treatment**. Fluorescence decay after photo activation for every construct. The cells were treated with 10 μM Colchicine for 30 minutes, H_2O was used as a control. Mean ± standard error, n = 13-17 (**A**). Down to three remaining repeats a increase of FDAP can be observed. Association rate k^*_{on} and (**B**, displayed as decadic logarithm) and dissociation rate k_{off} (**C**)

plained by the lower number of binding partners due to microtubule destabilization. While the association rate for Δ369 is unaffected by Colchicine treatment, it is even higher for Δ338. Taking the error estimation in account it is not possible to formulate any differences in the association rate of Δ307 with or without Colchicine treatment. The dissociation rate (Figure 4.5 C) of tau441wt is unaffected by Colchicine treatment of the cells. Interestingly the dissociation rate for tau352wt is lower after treatment with Colchicine than it is in the carrier control. As we postulated that tau352wt is interacting more frequent with microtubules (see 4.1.1) it is also more likely to be affected when altering microtubule dynamics. In the boundaries of the error estimation there is no difference between Colchicine treatment and carrier control for the Δ307, while there is a very small difference in Δ369. There is a very high difference between Colchicine treatment and carrier control for cells that are transfected with the Δ338 fragment.
To see if stabilization of microtubules on the other side would have an influence on tau dynamics we treated the cells with Epothilone D (EpoD). Epothilones are a group of substances with five subspecies (Epothilone A-F) that are considered to be of great use in cancer treatment. They stabilize microtubules by a similar mechanism like Paclitaxel (also known as *Taxol*). Epothilone D binds to the Paclitaxel-binding site [22]. This site is located at the β-subunit of the $\alpha\beta$-tubulin heterodimer [58, 63]. By Binding it decreases the rate of $\alpha\beta$-tubulin dissociation. The EpoD stocks were dissolved in dimethyl sulfoxide (DMSO) and then diluted in ddH_2O, so we used the same relative amount of DMSO (0.001%) solved in water as a control. After four days of NGF treatment we treated the transiently transfected PC12 cells with 1 nM EpoD or DMSO control for 30 minutes. Imaging was performed for no longer than an hour so the cells were exposed to EpoD for not longer than 90 minutes. Figure 4.6 A shows that stabilizing the microtubules with Epothilone D has no significant effect on FDAP of both wild type isoforms 441 and 352 or the microtubule interacting fragments compared to the DMSO control and also Δ307 and 3×PAGFP control are not affected. Nevertheless there are differences in the association rate (Figure 4.6 B) of tau352wt and Δ369 and Δ338, where the association rate is slightly higher for Epothilone D treated cells than for the DMSO control. The increase of the association rate after Epothilone D treatment of cells transfected with tau352wt, Δ369 and Δ338 is coupled with a slight increase of dissociation rate (Figure 4.6 C). The effect is biggest for Δ338, but overall very little (0.01 to 0.03 s^{-1}) so we conclude from these results that tau interaction with microtubules is unaffected by stabilizing microtubules with EpoD. This leads to the conclusion that stabilizing microtubules and therefore providing more binding partners does not lead to more binding of tau to microtubules.

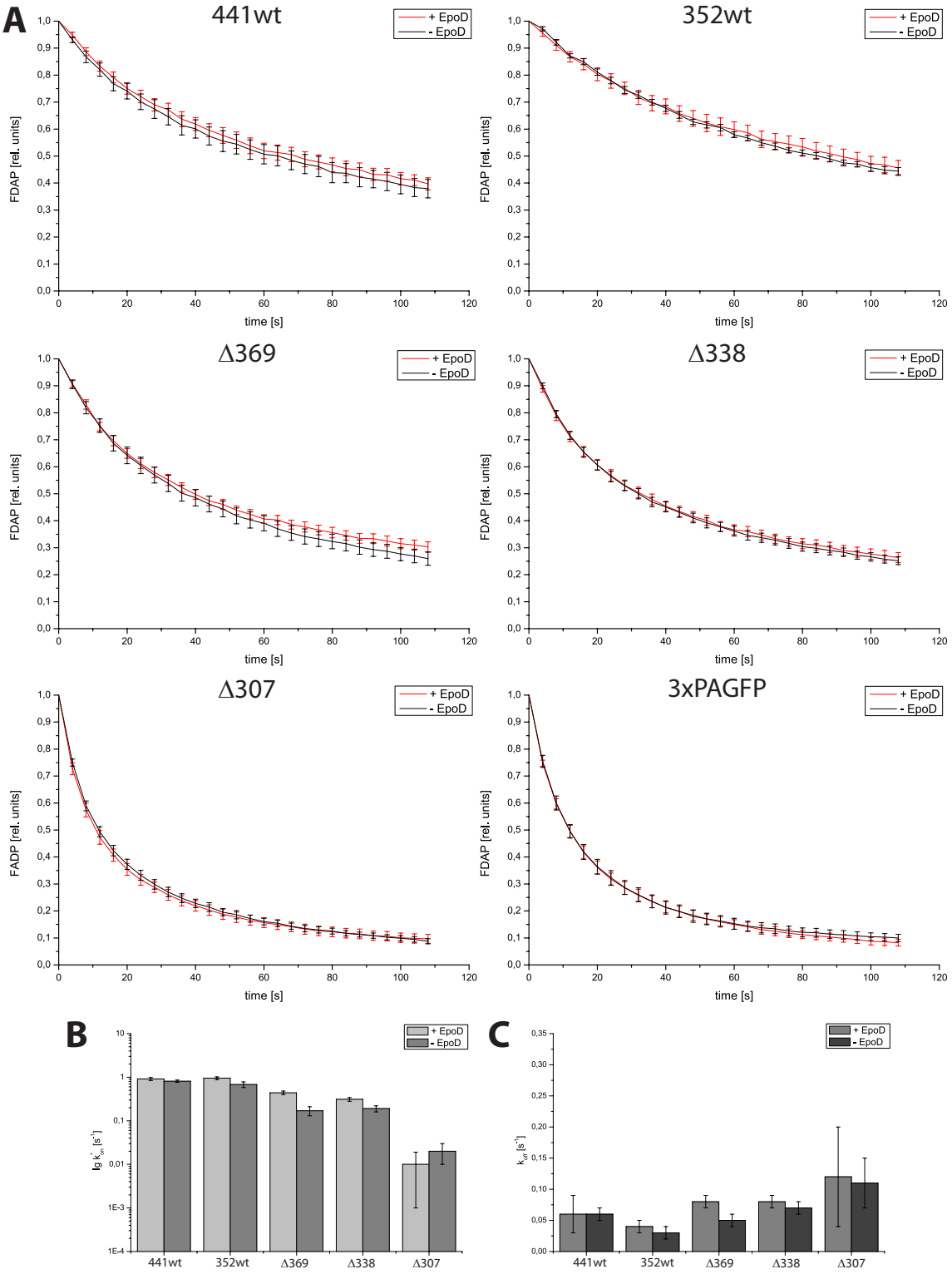

Figure 4.6: **FDAP and association and dissociation rates of tau and its fragments in the middle of the process with and without Epothilone D treatment**. Fluorescence decay after photo activation for every construct. The cells were treated with 1 nM EpoD for 30 minutes. 0.001% DMSO was used as a control. Mean ± standard error, n = 8-14 (**A**). No difference between the Epothilone D treated cells and the control can be observed. Association rate k^*_{on} (**B**, displayed as decadic logarithm) and dissociation rate k_{off} (**C**)

There are certain differences in association rates for ddH_2O control and DMSO control. Especially for tau352wt these differences are observable; while the association rate of tau352wt is 3.89±0.01 s^{-1} for ddH_2O control, it is 0.68±0.01 s^{-1} for DMSO control. Also the dissociation varies in cells transfected with tau352wt (0.14±0.01 s^{-1} for ddH_2O control, 0.03±0.01 s^{-1} for DMSO control). In other studies we also encountered the fact that DMSO has an influence on microtubule dynamics and seems to stabilize microtubules. The reason for this effect still has to be determined.

4.1.3 Influence of Phosphorylation on Interaction of Tau and its Fragments with Microtubules

Phosphorylation of tau can affect the tau-microtubule interactions in multiple ways [7, 45]. Previous studies showed that glutamate substitution can simulate hyperphosphorylation of tau protein [23] and a series of phosphorylation-mimicking serine/threonine to glutamate exchanges in the P-region is sufficient to block nucleation with microtubules *in vitro* [24]. To test the effect of pseudophosphorylation on tau dynamics and microtubule interaction, we used a PAGFP-tagged tau 441 construct that mimics phosphorylation by exchanging the amino acids serine 198, 199, 202, 235, 396, 404, 409, 413, 422 and threonine 231 to glutamate and tagged them to PAGFP (see figure 4.7). From this we constructed a pseudohyperphosphorylated version of our Δ369 fragment construct by inserting a stop codon after amino acid 369.

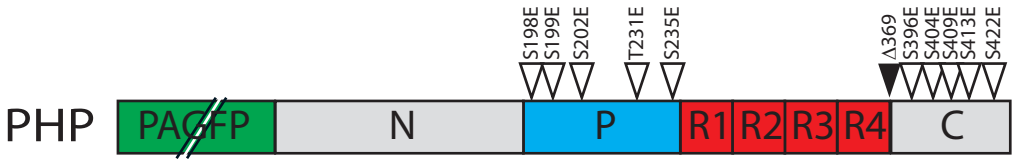

Figure 4.7: **Phosphorylation-mimicking tau fragments.** Tau441wt was used to create a pseudohyperphosphorylated (PHP) form of tau. White arrows show mutations to glutamate to mimic phosphorylation. Black arrows indicate mutations to truncate full length tau to specific truncation products.

The cells were transiently transfected with PAGFP-tagged and the PHP full length tau and PHP-Δ369 fragment. After 4 days of NGF treatment imaging was performed. We photoactivated was performed in the middle of the processes. When we compare PHP-tau441 with its wild type we see no significant increase or decrease of FDAP altough there is a small difference between the two curves. Also

for the Δ369 fragment there is no significant difference between the curves of the PHP and the non-PHP form; we reason that the mobility of tau in the cells was not affected by pseudohyperphosphorylation.
When we look at the association rates thought (Figure 4.8 B) we can see a decrease of k^*_{on} for the pseudophosphorylated tau and its fragment compared to their counterparts. The association rate of tau441 is lowered by a factor of 2.5 (from 6.2±0.3 s^{-1} for the wild type to 2.5±0.07 s^{-1} for the PHP construct) and for Δ369 it is even lowered by a factor of 10 (from 1.5±0.05 s^{-1} for Δ369 to 0.15±0.03 s^{-1} for PHP-Δ369). So pseudophosphorylation has a strong negative effect on tau's ability to attach to the microtubule surface. It also has an effect on the dissociation rate (Figure 4.8 C), for k_{off} is decreased for both PHP-tau441 and PHP-Δ369. Although the difference is much smaller than for k^*_{on}, it is a notable observation that the k_{off} rates of both PHP-constructs are the same (0.09±0.002 s^{-1} for PHP-tau441 and 0.1±0.01 s^{-1} for PHP-Δ369). So in this case pseudophosphorylation leads to a decrease and an equalization of the dissociation rate which means that pseudohyperphosphorylated tau tends to stay attached longer to the microtubule surface. The decreased association combined with the tendency to more likely keep in contact with microtubules results in a very small chance in FDAP and therefore in the overall mobility.

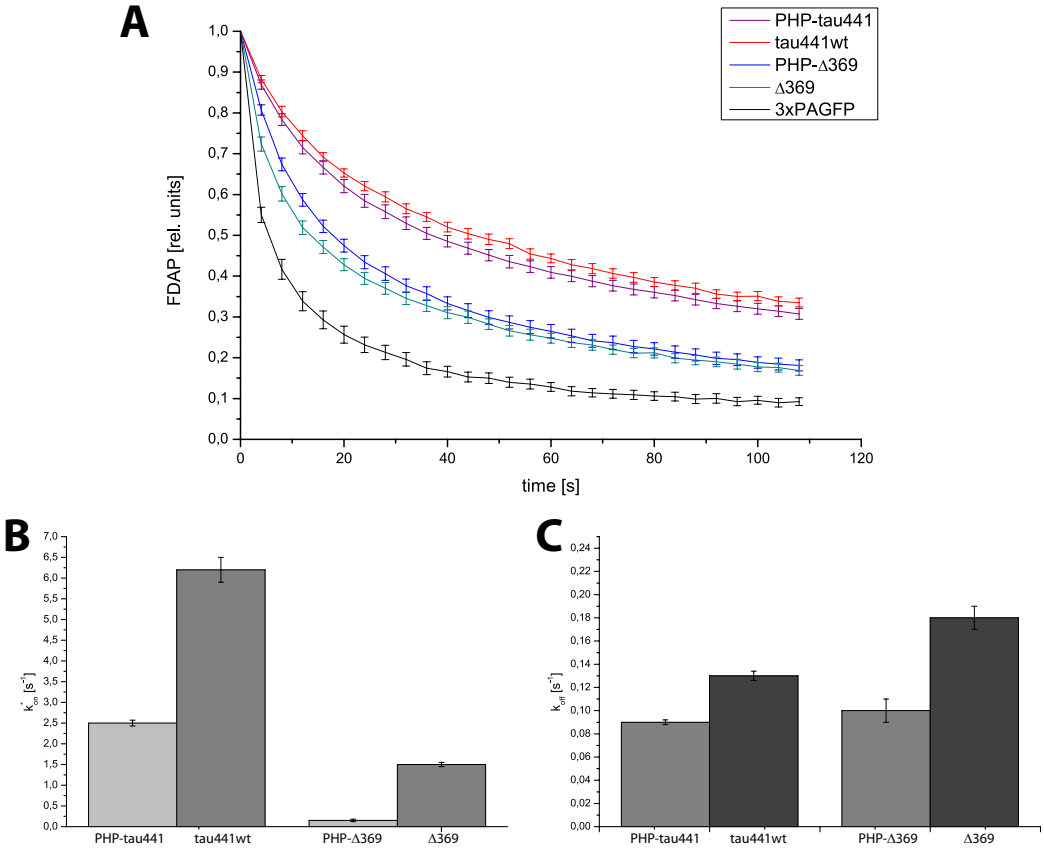

Figure 4.8: **Influence of phosphorylation on tau's mobility**. No significant difference in FDAP can be found between tau441wt and PHP-tau. The same can be observed for Δ369 and its pseudophosphorylated form PHP-Δ369. Mean ± standard error, n = 16-17 (**A**). The association rate k^*_{on} is decreased for phosphorylated forms of tau441wt and its fragment (**B**). The same decrease is also observable for the dissociation rate k_{off} (**C**).

4.2 Caspase cleavage and cleavage-like products

Studies show that proteolysis of tau by Caspase 3 at aspertate 421 is associated with NFTs in the brains of Alzheimer disease patients [6]. Caspase 3 is a protease that is activated during the execution phase of cell apoptosis [35]. Interestingly this naturally cleaved fragment seems to appear even before apoptosis [27]. Also, little is known so far about the function of the carboxyterminal part of tau protein where the cleavage site is located. We were interested in the effect that this truncation in the c-terminal part has on the mobility and microtubule-interaction of of tau protein. We created a product that is mimicking the caspase 3 cleavage by inserting a stop codon after aspertate 421, leading to a shortened tau protein expression that has the same length than the cleaved tau (Figure 4.9). We tagged it to PAGFP so we could perform live cell imaging with this fragment. We also created a second, caspase cleavage-like fragment with only 401 amino acids. Older studies state the existence of a R' that has only a low homology and is usually not considered as a repeat, but is stated to play a role in microtubule targeting [34]. To address this, we created this Δ401 fragment that stops after this R' and therefore is even 20 amino acids shorter than our Δ421 construct.

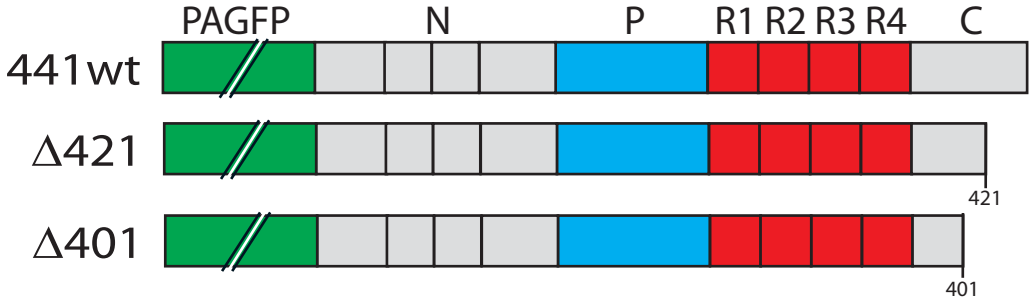

Figure 4.9: **Caspase cleavage and cleavage-like fragments** Full-length (441) tau was truncated via site directed mutagenesis by inserting a stop-codon after aspartate 421 (Δ421) or after glycine 401 (Δ401).

The cells were transiently transfected with either the PAGFP-tagged Δ421 or Δ401 fragment and treated with NGF for four days after transfection. Imaging was performed afterwards and photoactivation was conducted in the middle of the processes. Removing the last 20 amino acids of tau441wt leads to a decrease of FDAP (Figure 4.10 A) which states that Δ421 is less mobile than full length tau. The smaller fragment Δ401 shows an even more decreased fluorescence decay. So removing the c-terminus of tau highly affects the mobility of tau by slowing it down. Statistic analysis showed that the decrease of FDAP for Δ421 and Δ401 compared to tau441wt and also the difference between the FDAP of Δ421 and Δ401 are significant (table 4.4). The fragments show a reduced tendency to bind

Table 4.4: **Statistical analysis of FDAP of caspase cleavage and cleavage like fragments.** Significance was calculated using One way ANOVA (P<0.05) for FDAP values at 10 and 50 seconds. + indicates that the curves are significantly different in both values, - means no significant difference. The respective curves can be seen in figure 4.10.

	441wt	Δ421	Δ401
441wt		+	+
Δ421	+		+
Δ401	+	+	

Table 4.5: **Derived bound rates for caspase cleavage and cleavage-like fragments**. Truncation of carboxy-terminal amino acids leads to an increase of the bound fraction. Standard errors are shown below each value. n = number of cells

	441wt	Δ421	Δ401
Bound fraction	98%	99%	99%
SE	0.15	0.26	2.39
n	15	23	17

to microtubules, according to the association rates (Figure 4.10 B). While k^*_{on} is 6.2±0.3 s^{-1} for tau441wt, the rate drops to 2.8±0.2 s^{-1} for Δ421 and 1.5±0.4 s^{-1} for Δ401. But it also has an effect on the dissociation rate (Figure 4.10 B), that is also reduced for the caspase cleavage and cleavage-like fragments. While k_{off} is 0.13±0.004 s^{-1} for tau441wt, it id reduced to 0.03±0.002 s^{-1} for Δ421 and even to 0.008±0.002 s^{-1} for Δ401. Removing 20 to 40 amino acids from the c-terminal part of tau therefore reduces its tendency to detach from microtubules once it has bound, which matches the observation of decreased mobility and therefore a decreased FDAP. From the association and dissociation rate we are able to derive the fraction of microtubule-bound tau for these fragments (table 4.5). The data show that caspase cleavage and caspase cleavage-like fragments have a bigger fraction of microtubule bound tau, which can be explained by the lower k_{off} and therefore the lower tendency to dispatch from microtubules once bound, despite the lower association rate.

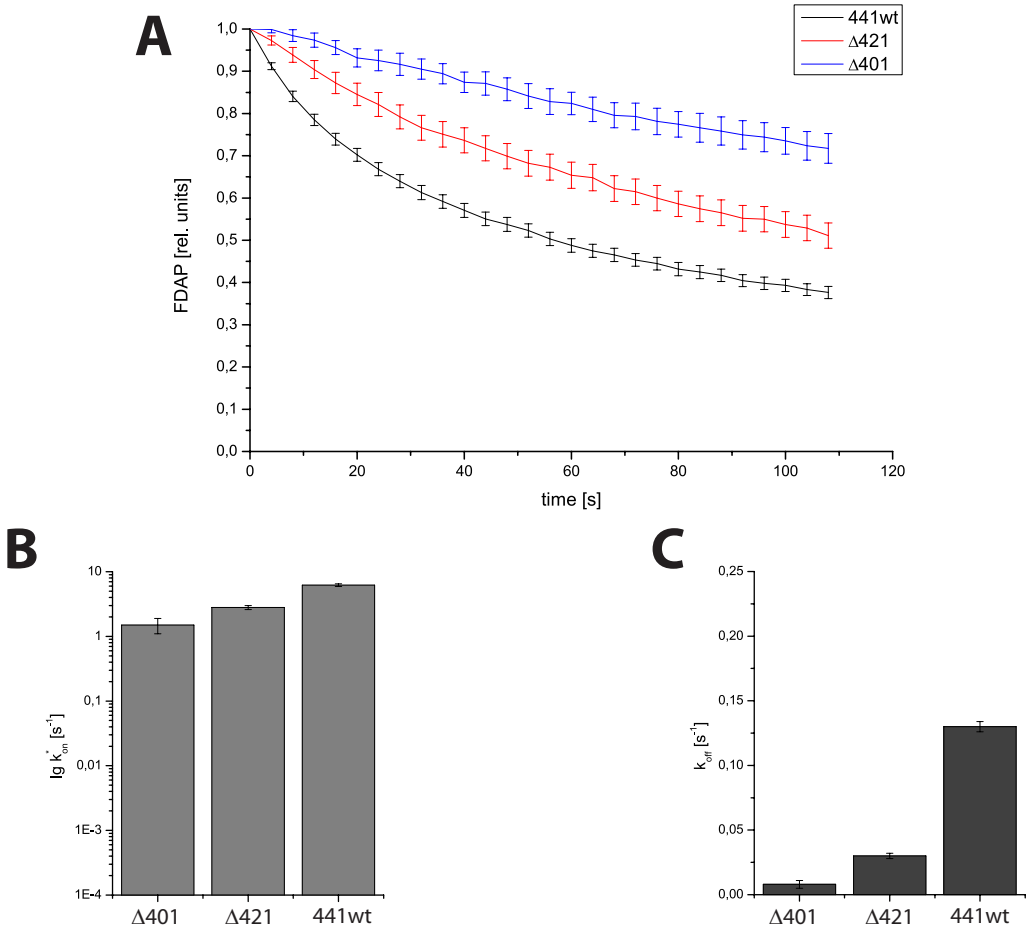

Figure 4.10: **Fluorescence decay after photoactivation for Caspase cleavage and cleavage-like tau fragment**. The fragment mimicking the Caspase3 cleavage product shows a lower fluorescence decay than wildtype tau. By shortening the carboxy-terminal part even more by using a fragment that stops after amino acid 401, this effect can be increased. Mean ± standard error, n = 15-23 (**A**). Both association rate k^*_{on} (**B**, shown as decadic logarithm) and dissociation rate k_{off} (**C**) are decreased.

4.3 Effect of tau on microtubule stability

After we examined the influence that the repeat domains of tau have on its mobility and microtubule interaction, we wanted to address tau's role in microtubule stability. Tau stabilizes microtubules by binding to the microtubule surface and promote their self-assembly from tubulin subunits [42, 49]. To address this, we transiently transfected PAGFP-tagged α-tubulin into PC12-cells and afterward treated them with NGF for four days. The marked α-tubulin would be integrated into the tubulin dimers and eventually into the microtubules (Figure 4.11 A). The fraction of PAGFP-α-tubulin that is integrated into microtubules is assumed immobile, while the unbound fraction can diffuse. By activating a small population of the tagged tubulin in the middle of the process and observing the FDAP in the activation region, we can draw conclusions about the ratio of bound to free tubulin

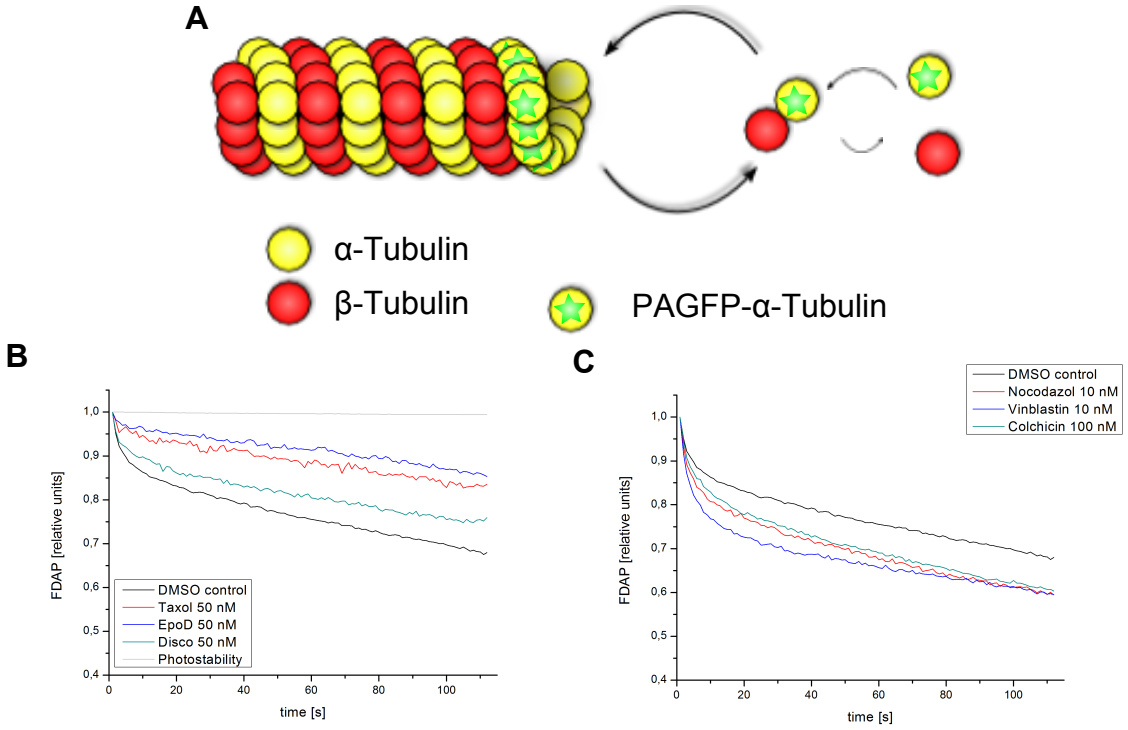

Figure 4.11: **PAGFP-tagged α-tubulin is integrated in microtubule dynamics**. PAGFP-α-tubulin forms dimers together with β-tubulin. These dimers take part in microtubule assembly and disassembly in form of a dynamic instability. This results in a bound dimer fraction and a unbound fraction (**A**). Treatment with microtubule stabilizing agents Paclitaxel (*Taxol*), Epothilone D (*EpoD*) and Discodermolide (*Disco*) (**B**) lead to a decreased FDAP in the region of photoactivation while treatment with destabilizing agents Nocodazole, Colchicine and Vinblastine (**C**) increases the fluorescence decay. Treatment was performed for 30 minutes with the respective agents or with 0.01% DMSO control. Photostability was unaffected. n = 17-26.

and therefore about the stability of microtubules. We tested this approach with different substances. All substances were dissolved in DMSO and diluted with water. The final DMSO concentration was 0.01%, as a control we used DMSO dissolved in water. The cells were treated for 30 minutes with the respective substance, afterwards imaging was performed for maximum 60 minutes. Paclitaxel (also known as *Taxol*), Epothilone D and Discodermolide are reducing microtubule disassembly and therefore stabilize microtubules. In our assay this leads to a higher fraction of photoactivated PAGFP-tagged α-tubulin in the activation region and therefore to a decreased FDAP (Figure 4.11 B). Nocodazol, Vinblastine and Colchicine on the other hand are destabilizing microtubules by binding to tubulin-dimers and prevent their assembly to microtubules, which leads to an increased FDAP (Figure 4.11 C).

We used a lenti virus infection system to express tau in PC12 cells. The viral vector had a CaM kinase II promoter that is neuron specific and has a lower expression level than it is with the CMV promoter, also Lenti virus integrates into the genome, leading to a more stable, longer lasting expression. To verify tau expression in our PC12 cell model system, we created a mCherry-tau441wt construct. To see if the higher binding affinity of caspase cleaved tau (see 4.2 on page 51) has any influence on microtubule stability, we also created a mCherry-tagged tauΔ421. We used 3×mCherry, consists of three copies of mCherry linked together to one molecule, as a control protein. Twelve days before imaging we infected the cells with tau, the caspase cleavage fragment or the control. Six days before imaging we transiently transfected the cells with PAGFP-α-tubulin. Four days before imaging we treated them with NGF to promote differentiation. For imaging we chose cells that showed red fluorescence and green fluorescence to which we referred as "double" and cells that only showed green fluorescence we referred to as "control" (Figure 4.12). All cells however, double and control, were from the same dish to exclude the possibility that differences in the results could be an effect of differences in conditions of culturing due to infection with lenti virus. We performed 3 independent experiments for each construct and summed up the results.

Expressing mCherry-tau441wt in PC12 cells leads to a decrease of FDAP of α-tubulin in the activated (Figure 4.13 A). Expression of the cytosolic non-interacting control protein 3×mCherry on the other hand shows no significant difference in FDAP between "double" and "control" cells (Figure 4.13 B). So α-tubulin is distributed significantly slower in the cell in the presence of human mCherry-tagged full-length tau. This indicates a bigger fraction of polymerized tubulin dimers which leads to the conclusion that human tau441wt has a stabilizing effect on microtubule dynamics in the processes of PC12 cells. For cells expressing

mCherry-tagged Δ421 a decrease of FDAP was observed in comparison to the respective control cells (Figure 4.13 C). However the difference between control and double in mCherry-Δ421 cells is not visibly higher than in mCherry-tau441wt expressing cells and a difference between tau441wt and Δ421 can not be confirmed with this data.

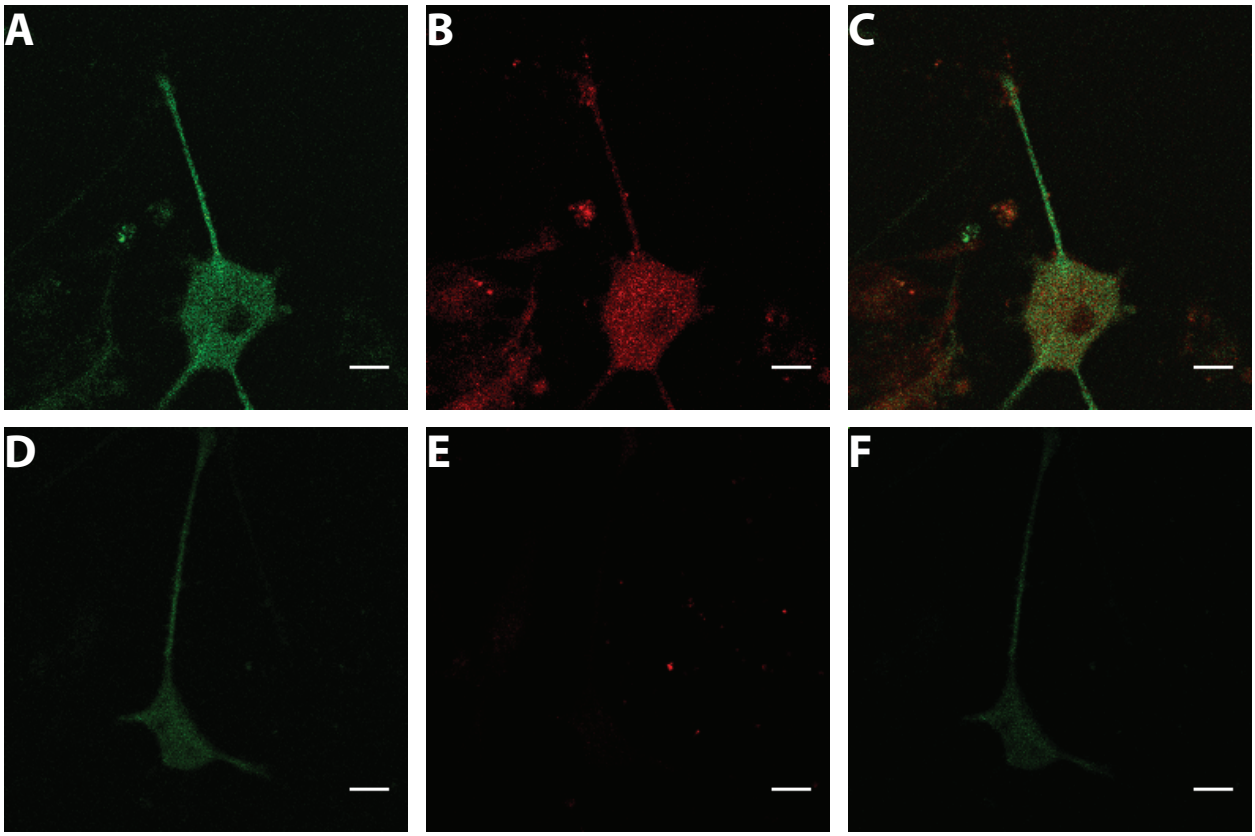

Figure 4.12: **Example for cells with two fluorescent markers (A-C) and control (D-F)**. Cells were infected via a lenti virus with a mCherry-tagged tau or a 3×mCherry-construct (as in this example) and transiently transfected with PAGFP-αTubulin. Cells that showed a fluorescence signal in the red channel and were positively transfected (green channel **A**, red channel **B** and overlay **C**) were defined as "double", cells that only were transfected but show no mCherry fluorescence (green channel **D**, red channel **E** and overlay **F**) were used as control. Both cells are from the same dish. Scale bar, 10 µm.

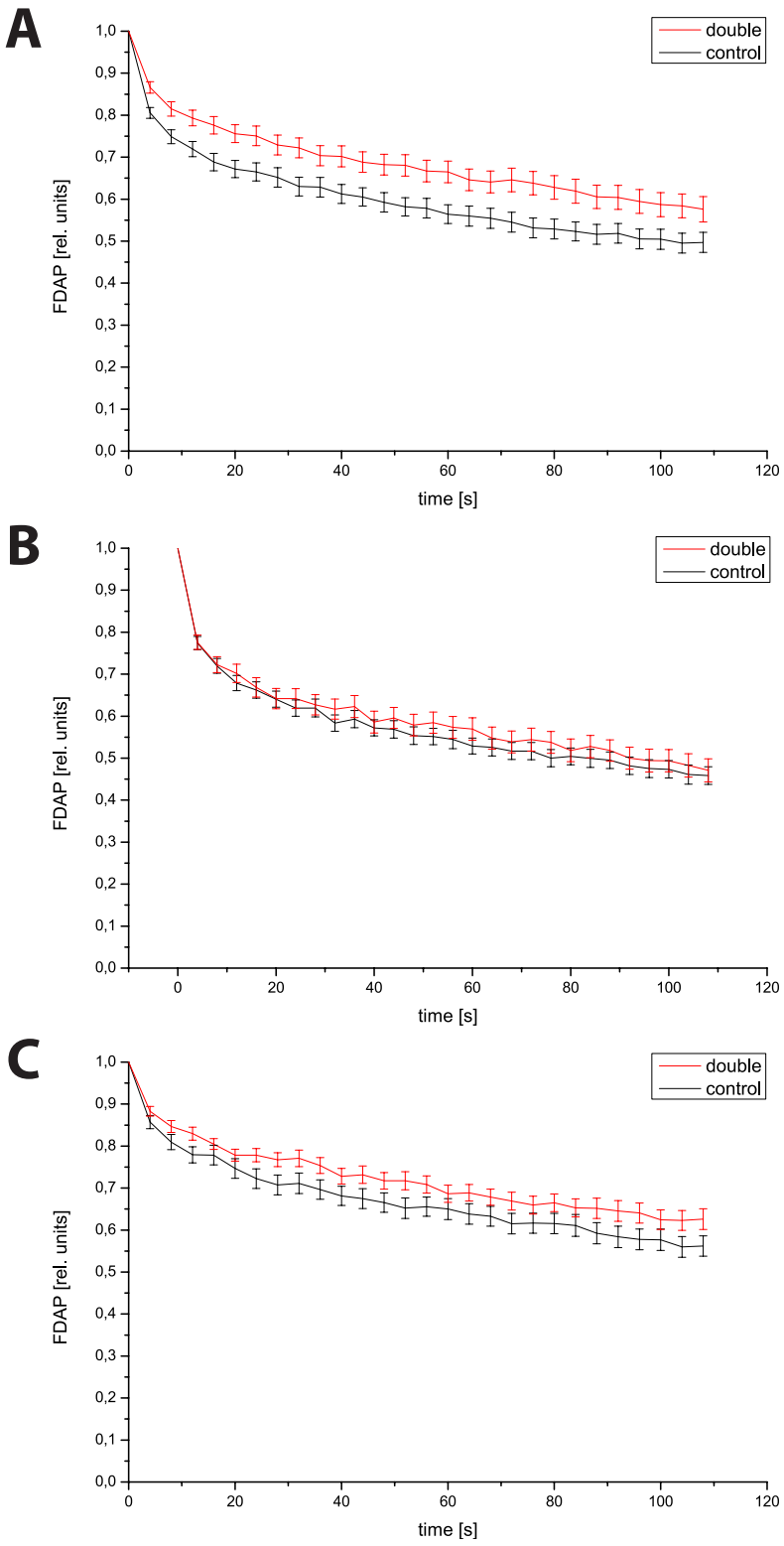

Figure 4.13: **Tubulin dynamics in cells that express mCherry constructs**. Cells expressing mCherry-tau441wt (**A**) show a significantly slower FDAP and therefore a slower αTubulin mobility than their respective, mCherry-negative control cells, whereas 3×mCherry expressing cells (**B**) show no significant difference to their control cells. mCherry-tauΔ421 expressing cells (**C**) show a slight difference to their controls. Mean ± standard error, n = 26-39.

5 Discussion

5.1 Structural factors of tau-microtubule interaction

Hence the fact that the repeat region is commonly seen as the microtubule-interacting part of tau [13, 43] our interest is focused on this particular region of tau's primary structure. By reducing the number of repeats via truncation from the c-terminal direction we hoped to see alterations in tau's mobility and therefore in its binding to microtubules. The increase of FDAP with decreasing numbers of repeats shows that the affinity of tau protein for microtubules *in vivo* is dependent on the total number of repeats. This is consistent with former *in vitro* studies [13]. We found out that when we cut off all repeats but two, fragments Δ276 and Δ307 show nearly the same FDAP than 3×PAGFP, which is our non-interacting control construct. If there is no interaction, the tau fragments can diffuse unhindered through the cell, just like our cytosolic control protein. (figure 4.2). From this we conclude that tau fragments with one or two repeats do not interact with microtubules (Δ276 appears to move even faster; to explain this one has to keep in mind that diffusion speed is connected to the hydrodynamic radius of a molecule. Since Δ276 only has 2/3 of the size of tau441wt and 3×PAGFP was chosen because its size is similar to that of tau441wt it is plausible that Δ276 has an even higher FDAP). So the minimal number of repeats required for microtubule binding is three. This corresponds to the native isoforms existing in the central nervous system, that also have at least three repeats. When we look at other Microtubule Associated Proteins (MAPs) we also can find microtubule binding regions consisting of a series of at least 3 repeats; both MAP2 and MAP4 contain a series of three 18 amino acids long peptides in their c-terminal part that are homologous to the motif present in tau [14, 44]. And there also exist isoforms of MAP2 with 4and MAP4 isoforms with up to 5 repeats [15, 41]. The microtubule binding domain of MAP1B on the other hand is unrelated to that of tau [54]. This loss of binding is also resembled in the diminishing association rates. The truncation of everything but the four repeats on the c-terminal sites already results in a reduction of k^*_{on} by a factor of 4 (k^*_{on} is 6.2 s^{-1} for tau441wt

and 1.5 s^{-1} for Δ369). That means that not only the repeats contribute to microtubule association, but also the c-terminal part of tau. Loss of another repeat and reduction to 3 repeats decreases the association rate again with a factor of 5 to 0.3 s^{-1} for Δ338. If we take account of the microtubule assembly is a result of the sum of binding affinities of single repeats, it is consistent that there is also a difference between a two-repeat and a one-repeat-fragment, although the association rates are very small for both. The k_{off}-rate is going up when removing the c-terminal part of tau, so without the last 72 amino acids the fragment is dissociating from microtubules more likely, which contributes to the higher mobility of the fragment. The fragments Δ307 and Δ276 show a similar k_{off}-rate than tau441wt, but the high error estimation and their k^*_{on}-rates shows us that this is due to the fact that these two fragments are not binding good to microtubules at all; a dissociation rate for a fragment that hardly binds at all must have a high variation and cannot be completely explicit. Δ338 on the other hand shows a decreased dissociation rate compared to the wild type. Its rate is also similar to Δ369f, so the decrease of k_{off} cannot fully explained by the specific repeats themselves: Both have 3 repeats left, their main difference is that Δ369f is missing repeat 2, while Δ338 lacks repeat 4. Also the presence or absence of exon 2 and 3 makes no difference in the dissociation rate. If we compare these two fragments with tau352wt, we see a decrease in the dissociation rate, wich also indicates that the c-terminal part also plays a role in microtubule interaction, an observation that was previously described *in vitro* [33]. In general tau352wt interacts more often with microtubules than tau441wt, represented by its higher k^*_{on} and k_{off} rate - this increase of both values explains the similarity of FDAP with full-length tau; a roughly proportional increase of both will compensate the effect on tau mobility (compare with equation 3.2 on page 34). So 352wt attaches and detaches more often, which fits to its occurrence in cell development. During a fetal stage, the cells undergo much development and rearrangements, also connected to changes in the cytoskeleton and therefore in microtubule structure. A tau isoform that attaches and detaches more often could support these rearrangements while in an adult organism a isoform that interacts more slowly may be needed to support microtubule structures in neuronal cells.

A feature of axons is that they show a strict polarity in microtubule organization. Also former studies show that tau tends to enrich in the distal part of axons of primary cortical cultures [70]. Therefore it was also important for us to look at tau's mobility at the tip of the processes of our PC12 model system. The main problem was the shape of the tip. Where the middle of the process can be considered a tube with two open endings where the proteins can diffuse in two different directions, the tip is a geometric construct with only one open end. Our algorithms for

determine association and dissociation rate would not fit. Also, proteins can only move into one direction after photoactivation, so our FDAP curves from photoactivation in the middle of the process are hardly comparable with the curves from tip activation. Nevertheless, the tendencies for the fragments stay the same with 3 repeats as minimum for tau-microtubule-interaction. One big differences to FDAP in the middle of processes is that the differences in FDAP in the tip get smaller and are no longer significant (compare table 4.3). Also the FDAP for tau441wt is similar in its immobile fraction (this is observable at later time points of the fluorescence decay, around 100 seconds). So for later time points the microtubule binding predominates shape-related effects. This effect gets lost with decreasing numbers of repeats and also for the control; at later time points, the fraction of 3×PAGFP in the activation region is higher for tip activation than for middle activation, and so it is for all other fragments. This effect is also slightly lower for tau352wt. As it attaches and detaches more frequently, a different shape is affecting its mobility more than that of full length tau. On the one hand this means that overexpression of human tau protein in mouse primary cortical neurons leads to a equal distribution of tau in the cell. On the other hand it shows that there is no compartment specific difference in tau-microtubule interaction in these cells.

When we compare our transiently transfected PC12 cell model with primary culture neurons infected with a lenti viral vector expressing PAGFP-tau441wt, we see no significant difference in FDAP between a process in a PC12 cell and an axon or dendrite in a neural cell, but the apparent association rate is higher, leading to the conclusion that tau binds less frequent to microtubule. Here we have to keep in mind that we are calculating the *apparent* association, which is defined as product of the association rate k_{on} and the free binding partners in an equilibrium state (see equation 3.4 on page 34). So if the number of binding partners in primary cultures differ from PC12 cells *in vivo*, the calculated k^*_{on} would be also different. The far more interesting observation is that when we express human tau in a neural cell via lenti virus, there is no significant difference in FDAP in the different compartment: Tau mobility seems to be equal in axons and dendrites. Also the k^*_{on} rates of axons and dendrites do not differ, leading to the conclusion that the mobility of lenti viral expressed, PAGFP-tagged tau441wt is the same in axons and dendrites. This is interesting because tau is not known to be equally distributed in neuronal cells, but found mostly in the axons [30].

The next question we tried to address is the influence of altered microtubule dynamics on tau mobility. Various substances are known to affect the dynamic instability of microtubule assembly and disassembly and a lot of them are used in cancer treatment. We already found out that truncation of tau and reduc-

tion of the number of repeats increases mobility and decreases microtubule-interaction by reducing its association and dissociation rates. By using Colchicine and Epothilone D we want to combine changes on tau and microtubule stability. As expected, changes in tau FDAP and therefore in mobility after colchicine treatment only occurred for tau fragments that are actually still able to bind to microtubules. That means that for Δ307 we had the same FDAP as for the non-interacting control construct 3×PAGFP. Also its k^*_{on} and k_{off} rate are not altered. We see a significant effect on colchicine treatment on the FDAP of tau441wt we attribute to the reduced number of possible binding partners due to the destabilization of microtubules. This is also backed by a decreased k^*_{on} rate combined with no alteration of the k_{off} rate; while tau441wt does not bind so often to microtubules when they are destabilized and a lower number of binding partners is available, it still detaches with the same rate once it is interacting with microtubules. We see a different effect when we look at the mobility of Δ338. Here the FDAP is also higher than in the carrier control, especially at earlier time points. At later time points the curve converges to the curve of the control. The association rate of Δ338 is higher than for the carrier control which means that it binds more often to microtubules, but according to the dissociation rate it also detaches more often. So by reducing the number of repeat and destabilizing microtubules and therefore also reducing the binding sites the interaction is altered in a new way that differs from full length tau. The smallest effect is visible for Δ369. The FDAP is slightly higher, although the association rate is not different after colchicine treatment compared with carrier control and the dissociation rate is only slightly higher. Also tau352wt shows a slight increase of the FDAP. Analog to tau441wt, the association rate is decreased after colchicine treatment. In contrast to tau441wt the dissociation rate is slightly higher for tau352wt.
Epothilone D treatment on the other hand seems to have no influence on FDAP and therefore on tau mobility. The curves show no difference for Epothilone D treatment compared to DMSO control. Also the association rate of tau441wt shows only a very small difference with a slightly higher rate after Epothilone D treatment in compare to DMSO control. For the fragments the difference is much higher though. Δ369 shows an increase from $0.17 \pm 0.04\ s^{-1}$ for the DMSO control to $0.44 \pm 0.04\ s^{-1}$ after Epothilone D treatment and also Δ338 has a higher k^*_{on} rate after Epothilone D treatment than with DMSO control. Only Δ307 shows no difference, but as mentioned this fragment has not enough repeats to properly interact with microtubules any more. We also can observe a higher k^*_{on} after Epothilone D treatment for tau352wt. This leads to the idea that stabilization of microtubules could increase the number of binding sites for tau and thus make it easier to interact with the microtubule surface. But since the effect is very

small for full length tau the affinity of tau isoforms with four repeats for binding to microtubules is already close to its optimum, while for the fragments and for fetal tau stabilization can increase this affinity. While increase of the k^*_{on} rate after Epothilone D treatment is apparent, there is no distinct difference for the k_{off} rate between Epothilone D treatment and DMSO control. Differences are all within the error estimations, although there is a slight trend for a higher k_{off} rate after Epothilone D treatment for the tau fragments, but the difference is too small to derive any effect from this. It is more likely that stabilizing the microtubules has no effect on tau dissociation - Analog to the association rate of full length tau we can conclude that tau dissociation is already at its optimum and stabilizing does not increase this any more. This finding is contradictory to newer studies that state that microtubule modifications have substantial effects on the accessibility and/or the three-dimensional structure of the binding loci of tau with the microtubule surface [11].

As already mentioned in the beginning, phosphorylation affects tau-microtubule-binding. Microtubule assembly depends partially on the phosphorylation state of tau [45]. We tried to address this by using pseudohyperphosphorylated forms of tau protein and its fragments. Former studies showed that exchanging specific serines and threonines with glutamate can result in a model system to simulate hyperphosphorylation [23–25]. We used this system to look at the differences in tau mobility and tau-microtubule interactions with and without pseudohyperphosphorylation and in combination with our fragments. Surprisingly the results show no significant difference in tau mobility: The FDAP curves are nearly the same for the PHP constructs and their non-phosphorylated counterparts. This is contradictory to former studies that show that pseudohyperphosphorylation directly lead to a redistribution of tau from the axon to the somatodendritic compartment [70]. Nevertheless we can see a clear difference in the association and dissociation rates, stating that phosphorylation indeed affects tau-microtubule-binding by decreasing the tendency of tau to bind to the microtubule surface. Maybe pseudophosporylation does not affect detaching so much, but decreases tau's ability to bind to microtubules and by that way leads to the distribution towards the axon as former studies state. The fact that pseudophosphorylation decreases k_{off} of both tau441wt and Δ369 to the same level could indicate that the level of influence that phosphorylation has on the dissociation of tau is limited to a certain point.

5.2 Contribution of the c-terminus to tau's affinity to bind to microtubules *in vivo*

Studies propose a model in which caspase activation cleaves tau to initiate tangle formation, then truncated tau recruits normal tau to misfold and form tangles [20]. Interestingly this cleavage appears to precede the nuclear events of apoptosis [27], so this caspase 3 activity seems not to be linked to the processes of programmed cell death but is triggered by something else. However the relevant part for this study is whether caspase cleavage has any influence on tau-microtubule-interaction that precedes the formation of neurofibrillary tangles. In other words: Is caspase cleaved tau more likely detach from the microtubule surface or otherwise? Our results show that removing the last 20 or 40 amino acids from the c-terminal part of tau does decrease the fluorescence decay after photoactivation of tau fragments and not only affects its association rate but also the dissociation rate to this effect that tau is stronger attached to the microtubule surface and therefore its mobility is decreased. The derived binding rates state that the bound fraction of tau is higher for the Δ421 and Δ401 fragment than for tau441wt. Maybe this increased tendency to bind makes the caspase cleavage fragment Δ421 more likely to initiate tangle formation and to recruit normal tau. What is also very interesting is the question what role the c-terminal part plays in tau-microtubule-interaction. While removing the whole c-terminus up to the last repeat (so the last 72 amino acids) increases the mobility of the fragment and leads to a lower fraction of microtubule-bound tau, the removal of only the last 20 amino acids leads to a decreased mobility and a higher fraction of bound tau fragment. And the mobility is even more decreased for a fragment lacking the last 40 amino acids. Removing amino acids 369 to 401 has no further effect on the association rate (Δ369 and Δ401 have the same k^*_{on} rate), but there is a difference in the k_{off} rates (441wt: $0.13 \pm 0.004\,s^{-1}$, Δ369: $0.18 \pm 0.01\,s^{-1}$, Δ421: $0.03 \pm 0.002\,s^{-1}$, Δ401: $0.008 \pm 0.003\,s^{-1}$). So this leads to the assumption that the last 40 amino acids are involved in the detaching of tau from the microtubule surface. A lack of this amino acids consequently leads to a stronger binding and a decreased dissociation rate. Interestingly the lack of the last 72 amino acids compensates that effect. This suggests that in the c-terminal part, there are regions that tend to prevent disassembly (presumably in the amino acids 370 to 401) and others that deregulate this effect (localized in amino acids 402 to 441). Studies state the existence of a low homology region called "R'" which is usually not considered as a repeat, but is stated to play a role in microtubule targeting [34]. From our data we can derive that this region might have the effect to

influence microtubule binding, but not in a sense of targeting, but by increasing the persistence of the binding. The effect of this region might be countered by the last 40 amino acids of the c-terminus. This also could explain why removing only 20 amino acids (as in case of caspase cleavage) leads to partial compensation of this binding effect. Studies also showed *in vitro*, that the carboxy-terminal sequences downstream of the repeat region make a strong but indirect contribution to microtubule binding [33].

5.3 Influence of tau on the dynamic instability of microtubules

Microtubule-associated proteins like tau are characterized functionally by their ability to promote the assembly and stability of microtubules in axons and dendrites [30]. So to take a closer look at microtubule stabilization by tau expression, we developed an assay that could make stabilizing and destabilizing effects on microtubules visible with our microscopy set-up. To combine it with our live cell imaging assay, we used PAGFP-tagged α-tubulin. We chose α- over β-tubulin because β-tubulin tends to be cytotoxic when overexpressed. Experiments from our group show that this PAGFP tagged tubulin is still integrating into microtubules in sufficient amounts, so that we can draw conclusions about the changes in assembly and disassembly of tagged tubulin dimers in microtubules.
With this approach we are able to determine the stabilizing and destabilizing effect of substances on the dynamic instability of microtubules. We tested it with multiple known substances that have either a stabilizing or destabilizing effect on microtubules and were able to differentiate between those effects compared with a carrier control. We were also able to rule out photo bleaching effects as shown in figure 4.11 B: The overall intensity of each frame was constant, so the fluorophore was stable and not underlying any bleaching effect. What we had to keep in mind though was the effect of DMSO on microtubule stability. It turned out that this solvent had a stabilizing effect on our system. This shows that our model system is reacting very sensitive to changes and lead to the decision to image both double transfected and control cells from the same dish.
For expressing of the mCherry-tagged constructs we used a lenti viral infection system. It inserts the gene of interest stably into the genome of the target cells and has a CaM kinase II promoter with a moderate expression rate compared to the CMV promoter we used for the transient transfection. As a control construct we used - analog to our 3×PAGFP control - a 3×mCherry construct, which also

has roughly the same size like our mCherry-tau441wt constructs. Our experiments show that expressing a non-interacting protein in our PC12 cell system has no effect on FDAP and therefore on tubulin polymerisation (figure 4.13 B) so we can exclude effects on the dynamic instability of microtubules by just expressing another protein via lenti virus. The expression of mCherry-tau441wt on the other hand shows a decrease of FDAP in the activated region and therefore a lower mobility of tagged α-tubulin (figure 4.13 A). This shows us that human full length tau has an influence on microtubule stability and acts stabilizing, as described in the literature [30]. After we found out that caspase cleavage and cleavage-like tau fragments have a higher binding affinity to the microtubule surface, we also created a lenti viral vector for the mCherry-tagged tau fragment Δ421. We chose this fragment because it mimics a form of tau cleavage that actually can be observed in neural cells. If tau is stabilizing microtubules by binding to them and therefore prevent disassembly , a fragment that has a higher affinity to attach and stay attached to the microtubule surface will stabilize them even more. Despite our assumption, mCherry-tauΔ421 does lead to a decreased FDAP of PAGFP-tagged α-tubulin, but the effect is not higher than that of mCherry-tau441wt. This means that a fragment that has a higher tendency to stay at the microtubule surface has no higher stabilizing effect on microtubules. Therefore the idea that tau stabilizes microtubules by its binding to it can not be fully correct. We should take in account that tau is stabilizing microtubules not by its binding to it, but via a protecting effect. Studies suggest that tau prevents access of microtubule-seizing proteins like katanin and therefore stops these proteins from pulling out single tubulin units and cutting them that way [38, 57]. If we assume such a mechanism of "stabilization", it would be only dependent on the amount of expressed tau - a fragment with a higher affinity to bind would not make any difference in stabilization.

5.4 Outlook

Our results gave us a first insight in the functional organisation of the tau protein and the consequences for tau-microtubule-interaction. How this interaction actually works and what happens when tau descends into a pathological state is of great importance to get a deeper understanding in the processes that happen during tauopathies and especially during AD.
Our experiments gave us insight in the processes of tau mobility and microtubule interaction at the scale of tau populations, so our results base on the "behavior" of multiple molecules at once, where we are not able to resolve the behavior of

a single molecule. This gives us a kind of statistical stability as single molecules outliers do not distort our results that much, but to back up this results, experiments with single molecule tracking could be useful to see if the results we got from observing protein populations could also be reproduced on the level of single molecules. For the observations of tau mobility at the tip of a process we need a new model for determining the association and dissociation rates. Due to the different shape - the tip must be considered as a tube with only one open ending - new algorithms must be calculated for modeling and fitting. The determination of association and dissociation rate will give the opportunity to directly compare the differences of tau mobility in the tip and the middle of a process, for these parameters are independent of the shape. From the observation of the different fragments we can conclude that the ability of tau to interact with microtubules is not a effect of the respective repeats, but a product of the combined binding affinity of the repeats. Therefore it is not surprising that a minimum amount of repeats is needed for tau to bind to microtubules and that this number is also found in the natural isoforms of tau protein. However, we cannot address the role of the conformation of tau and structural influences on its interaction with microtubules with our approach. Tau is considered a intrinsically disordered protein [26, 39]. Nevertheless studies show that although these proteins do not exhibit any stable secondary structure in the free form, they are able to fold after binding to targets and contain regions with large propensity to adopt a defined type of secondary structure [62]. The comparison of the fragments Δ338 and Δ369*f* also suggests that the individual repeats don't play a role for themselves, but their total number and the structure of the protein. Our observations with the caspase cleavage and cleavage-like fragments also pose the question about the function of the carboxyterminus of tau and its role in binding to microtubules. Structural reasons that occur with the lack of the last 20 to 40 amino acids could affect the interactions and result in a fragment that does not detach so easily.
As our results show, a stronger binding tau construct does not have influence on microtubule stability. Taking the hypothesis in account that tau protects microtubules against microtubule-seizing proteins, further co-expression experiments could help to address this topic. When the protective effect is due to the fact that tau binds to microtubule and therefore hinders other proteins from seizing it, expression of fragments that have a weaker binding affinity for microtubules could have a lower stabilizing effect on microtubules - if they tend to bind less often and less good, they should also be less protective.

Literature

[1] J. Al-Bassam, R. S. Ozer, D. Safer, S. Halpain, and R. A. Milligan. MAP2 and tau bind longitudinally along the outer ridges of microtubule protofilaments. *The Journal of cell biology*, 157(7):1187–96, June 2002.

[2] a. C. Alonso, T. Zaidi, I. Grundke-Iqbal, and K. Iqbal. Role of abnormally phosphorylated tau in the breakdown of microtubules in Alzheimer disease. *Proceedings of the National Academy of Sciences of the United States of America*, 91(12):5562–6, June 1994.

[3] P. W. Baas, J. S. Deitch, M. M. Black, and G. A. Banker. Polarity orientation of microtubules in hippocampal neurons: uniformity in the axon and nonuniformity in the dendrite. *Proceedings of the National Academy of Sciences of the United States of America*, 85(21):8335–9, Nov. 1988.

[4] L. Bakota and R. Brandt. Live-cell imaging in the study of neurodegeneration. *International review of cell and molecular biology*, 276:49–103, Jan. 2009.

[5] M. Banerjee, D. Roy, B. Bhattacharyya, and G. Basu. Differential colchicine-binding across eukaryotic families: the role of highly conserved Pro268beta and Ala248beta residues in animal tubulin. *FEBS letters*, 581(26):5019–23, Oct. 2007.

[6] G. Basurto-Islas, J. Luna-Muñoz, A. L. Guillozet-Bongaarts, L. I. Binder, R. Mena, and F. García-Sierra. Accumulation of aspartic acid421- and glutamic acid391-cleaved tau in neurofibrillary tangles correlates with progression in Alzheimer disease. *Journal of neuropathology and experimental neurology*, 67(5):470–83, May 2008.

[7] J. Biernat, N. Gustke, G. Drewes, E. M. Mandelkow, and E. Mandelkow. Phosphorylation of Ser262 strongly reduces binding of tau to microtubules: distinction between PHF-like immunoreactivity and microtubule binding. *Neuron*, 11(1):153–63, July 1993.

[8] L. I. Binder, A. Frankfurter, and L. I. Rebhun. The distribution of tau in the mammalian central nervous system. *The Journal of cell biology*, 101(4):1371–8, Oct. 1985.

[9] R. Brandt and M. Hundelt. Tauopathy in Anzheimer's Disease. *Research Progress in Alzheimer's Disease and Dementia*, 3(541):1–15, 2007.

[10] R. Brandt, M. Hundelt, and N. Shahani. Tau alteration and neuronal degeneration in tauopathies: mechanisms and models. *Biochimica et biophysica acta*, 1739(2-3):331–54, Jan. 2005.

[11] G. Breuzard, P. Hubert, R. Nouar, T. De Bessa, F. Devred, P. Barbier, J. N. Sturgis, and V. Peyrot. Molecular mechanisms of Tau binding to microtubules and its role in microtubule dynamics in live cells. *Journal of cell science*, 126(Pt 13):2810–9, July 2013.

[12] L. Buée, T. Bussière, V. Buée-Scherrer, A. Delacourte, and P. R. Hof. Tau protein isoforms, phosphorylation and role in neurodegenerative disorders. *Brain research. Brain research reviews*, 33(1):95–130, Aug. 2000.

[13] K. A. Butner and M. W. Kirschner. Tau protein binds to microtubules through a flexible array of distributed weak sites. *The Journal of cell biology*, 115(3):717–30, Nov. 1991.

[14] S. J. Chapin and J. C. Bulinski. Non-neuronal 210 x 10(3) Mr microtubule-associated protein (MAP4) contains a domain homologous to the microtubule-binding domains of neuronal MAP2 and tau. *Journal of cell science*, 98 (Pt 1):27–36, Jan. 1991.

[15] S. J. Chapin, C. M. Lue, M. T. Yu, and J. C. Bulinski. Differential expression of alternatively spliced forms of MAP4: a repertoire of structurally different microtubule-binding domains. *Biochemistry*, 34(7):2289–301, Feb. 1995.

[16] M. F. Chau, M. J. Radeke, C. de Inés, I. Barasoain, L. A. Kohlstaedt, and S. C. Feinstein. The microtubule-associated protein tau cross-links to two distinct sites on each alpha and beta tubulin monomer via separate domains. *Biochemistry*, 37(51):17692–703, Dec. 1998.

[17] Z. Z. Chong, F. Li, and K. Maiese. Stress in the brain: novel cellular mechanisms of injury linked to Alzheimer's disease. *Brain research. Brain research reviews*, 49(1):1–21, July 2005.

[18] F. Clavaguera, T. Bolmont, R. A. Crowther, D. Abramowski, S. Frank, A. Probst, G. Fraser, A. K. Stalder, M. Beibel, M. Staufenbiel, M. Jucker,

M. Goedert, and M. Tolnay. Transmission and spreading of tauopathy in transgenic mouse brain. *Nature cell biology*, 11(7):909–13, July 2009.

[19] D. W. Cleveland, S. Y. Hwo, and M. W. Kirschner. Purification of tau, a microtubule-associated protein that induces assembly of microtubules from purified tubulin. *Journal of molecular biology*, 116(2):207–25, Oct. 1977.

[20] A. de Calignon, L. M. Fox, R. Pitstick, G. A. Carlson, B. J. Bacskai, T. L. Spires-Jones, and B. T. Hyman. Caspase activation precedes and leads to tangles. *Nature*, 464(7292):1201–4, Apr. 2010.

[21] A. de Calignon, M. Polydoro, M. Suárez-Calvet, C. William, D. H. Adamowicz, K. J. Kopeikina, R. Pitstick, N. Sahara, K. H. Ashe, G. a. Carlson, T. L. Spires-Jones, and B. T. Hyman. Propagation of tau pathology in a model of early Alzheimer's disease. *Neuron*, 73(4):685–97, Feb. 2012.

[22] V. Dostál and L. Libusová. Microtubule drugs: action, selectivity, and resistance across the kingdoms of life. *Protoplasma*, Mar. 2014.

[23] J. Eidenmüller, T. Fath, A. Hellwig, J. Reed, E. Sontag, and R. Brandt. Structural and functional implications of tau hyperphosphorylation: information from phosphorylation-mimicking mutated tau proteins. *Biochemistry*, 39(43):13166–75, Oct. 2000.

[24] J. Eidenmüller, T. Fath, T. Maas, M. Pool, E. Sontag, and R. Brandt. Phosphorylation-mimicking glutamate clusters in the proline-rich region are sufficient to simulate the functional deficiencies of hyperphosphorylated tau protein. *The Biochemical journal*, 357(Pt 3):759–67, Aug. 2001.

[25] T. Fath, J. Eidenmüller, and R. Brandt. Tau-mediated cytotoxicity in a pseudohyperphosphorylation model of Alzheimer's disease. *The Journal of neuroscience : the official journal of the Society for Neuroscience*, 22(22):9733–41, Nov. 2002.

[26] T. C. Gamblin. Potential structure/function relationships of predicted secondary structural elements of tau. *Biochimica et biophysica acta*, 1739(2-3):140–9, Jan. 2005.

[27] T. C. Gamblin, F. Chen, A. Zambrano, A. Abraha, S. Lagalwar, A. L. Guillozet, M. Lu, Y. Fu, F. Garcia-Sierra, N. LaPointe, R. Miller, R. W. Berry, L. I. Binder, and V. L. Cryns. Caspase cleavage of tau: linking amyloid and neurofibrillary tangles in Alzheimer's disease. *Proceedings of the National Academy of Sciences of the United States of America*, 100(17):10032–7, Aug. 2003.

[28] A. Gauthier and R. Brandt. Live cell imaging of cytoskeletal dynamics in neurons using fluorescence photoactivation. *Biological chemistry*, 391(6):639–43, June 2010.

[29] A. Gauthier-Kemper, C. Weissmann, N. Golovyashkina, Z. Sebö-Lemke, G. Drewes, V. Gerke, J. J. Heinisch, and R. Brandt. The frontotemporal dementia mutation R406W blocks tau's interaction with the membrane in an annexin A2-dependent manner. *The Journal of cell biology*, 192(4):647–61, Feb. 2011.

[30] M. Goedert, R. A. Crowther, and C. C. Garner. Molecular characterization of microtubule-associated proteins tau and MAP2. *Trends in neurosciences*, 14(5):193–9, May 1991.

[31] M. Goedert and M. G. Spillantini. A century of Alzheimer's disease. *Science*, 314(5800):777–81, Nov. 2006.

[32] M. Goedert, M. G. Spillantini, R. Jakes, D. Rutherford, and R. A. Crowther. Multiple isoforms of human microtubule-associated protein tau: sequences and localization in neurofibrillary tangles of Alzheimer's disease. *Neuron*, 3(4):519–26, Oct. 1989.

[33] B. L. Goode, M. Chau, P. E. Denis, and S. C. Feinstein. Structural and functional differences between 3-repeat and 4-repeat tau isoforms. Implications for normal tau function and the onset of neurodegenetative disease. *The Journal of biological chemistry*, 275(49):38182–9, Dec. 2000.

[34] N. Gustke, B. Trinczek, J. Biernat, E. M. Mandelkow, and E. Mandelkow. Domains of tau protein and interactions with microtubules. *Biochemistry*, 33(32):9511–9522, Aug. 1994.

[35] H. A. Harrington, K. L. Ho, S. Ghosh, and K. C. Tung. Construction and analysis of a modular model of caspase activation in apoptosis. *Theoretical biology & medical modelling*, 5:26, Jan. 2008.

[36] N. Hirokawa, Y. Shiomura, and S. Okabe. Tau proteins: the molecular structure and mode of binding on microtubules. *The Journal of cell biology*, 107(4):1449–59, Oct. 1988.

[37] K. Iqbal, A. D. C. Alonso, S. Chen, M. O. Chohan, E. El-Akkad, C.-X. Gong, S. Khatoon, B. Li, F. Liu, A. Rahman, H. Tanimukai, and I. Grundke-Iqbal. Tau pathology in Alzheimer disease and other tauopathies. *Biochimica et biophysica acta*, 1739(2-3):198–210, Jan. 2005.

[38] D. C. Jean and P. W. Baas. It cuts two ways: microtubule loss during Alzheimer disease. *The EMBO journal*, 32(22):2900–2, Nov. 2013.

[39] S. Jeganathan, M. von Bergen, E.-M. Mandelkow, and E. Mandelkow. The natively unfolded character of tau and its aggregation to Alzheimer-like paired helical filaments. *Biochemistry*, 47(40):10526–39, Oct. 2008.

[40] S. Kar, J. Fan, M. J. Smith, M. Goedert, and L. A. Amos. Repeat motifs of tau bind to the insides of microtubules in the absence of taxol. *The EMBO journal*, 22(1):70–7, Jan. 2003.

[41] S. Kindler and C. C. Garner. Four repeat MAP2 isoforms in human and rat brain. *Brain research. Molecular brain research*, 26(1-2):218–24, Oct. 1994.

[42] G. Lee. Tau protein: an update on structure and function. *Cell motility and the cytoskeleton*, 15(4):199–203, Jan. 1990.

[43] G. Lee, R. L. Neve, and K. S. Kosik. The microtubule binding domain of tau protein. *Neuron*, 2(6):1615–1624, June 1989.

[44] S. A. Lewis, D. H. Wang, and N. J. Cowan. Microtubule-associated protein MAP2 shares a microtubule binding motif with tau protein. *Science (New York, N.Y.)*, 242(4880):936–9, Nov. 1988.

[45] G. Lindwall and R. D. Cole. Phosphorylation affects the ability of tau protein to promote microtubule assembly. *The Journal of biological chemistry*, 259(8):5301–5, Apr. 1984.

[46] J. Lippincott-Schwartz and G. H. Patterson. Development and use of fluorescent protein markers in living cells. *Science (New York, N.Y.)*, 300(5616):87–91, Apr. 2003.

[47] F. Liu and C.-X. Gong. Tau exon 10 alternative splicing and tauopathies. *Molecular neurodegeneration*, 3:8, Jan. 2008.

[48] K. A. Lukyanov, D. M. Chudakov, S. Lukyanov, and V. V. Verkhusha. Innovation: Photoactivatable fluorescent proteins. *Nature reviews. Molecular cell biology*, 6(11):885–91, Nov. 2005.

[49] E.-M. Mandelkow and E. Mandelkow. Biochemistry and cell biology of tau protein in neurofibrillary degeneration. *Cold Spring Harbor perspectives in medicine*, 2(7):a006247, July 2012.

[50] M. D. Mukrasch, M. von Bergen, J. Biernat, D. Fischer, C. Griesinger, E. Mandelkow, and M. Zweckstetter. The "jaws" of the tau-microtubule interaction. *The Journal of biological chemistry*, 282(16):12230–9, Apr. 2007.

[51] S. Nath, L. Agholme, F. R. Kurudenkandy, B. Granseth, J. Marcusson, and M. Hallbeck. Spreading of neurodegenerative pathology via neuron-to-neuron transmission of β-amyloid. *The Journal of neuroscience : the official journal of the Society for Neuroscience*, 32(26):8767–77, June 2012.

[52] R. L. Neve, P. Harris, K. S. Kosik, D. M. Kurnit, and T. A. Donlon. Identification of cDNA clones for the human microtubule-associated protein tau and chromosomal localization of the genes for tau and microtubule-associated protein 2. *Brain research*, 387(3):271–80, Dec. 1986.

[53] H. Niwa, S. Inouye, T. Hirano, T. Matsuno, S. Kojima, M. Kubota, M. Ohashi, and F. I. Tsuji. Chemical nature of the light emitter of the Aequorea green fluorescent protein. *Proceedings of the National Academy of Sciences of the United States of America*, 93(24):13617–22, Nov. 1996.

[54] M. Noble, S. A. Lewis, and N. J. Cowan. The microtubule binding domain of microtubule-associated protein MAP1B contains a repeated sequence motif unrelated to that of MAP2 and tau. *The Journal of cell biology*, 109(6 Pt 2):3367–76, Dec. 1989.

[55] J. Nunez. Immature and mature variants of MAP2 and tau proteins and neuronal plasticity. *Trends in neurosciences*, 11(11):477–9, Nov. 1988.

[56] G. H. Patterson and J. Lippincott-Schwartz. A photoactivatable GFP for selective photolabeling of proteins and cells. *Science*, 297(5588):1873–7, Sept. 2002.

[57] L. Qiang, W. Yu, A. Andreadis, M. Luo, and P. W. Baas. Tau protects microtubules in the axon from severing by katanin. *The Journal of neuroscience : the official journal of the Society for Neuroscience*, 26(12):3120–9, Mar. 2006.

[58] S. Rao, G. A. Orr, A. G. Chaudhary, D. G. Kingston, and S. B. Horwitz. Characterization of the taxol binding site on the microtubule. 2-(m-Azidobenzoyl)taxol photolabels a peptide (amino acids 217-231) of beta-tubulin. *The Journal of biological chemistry*, 270(35):20235–8, Sept. 1995.

[59] D. P. Rice, P. J. Fox, W. Max, P. A. Webber, D. A. Lindeman, W. W. Hauck, and E. Segura. The economic burden of Alzheimer's disease care. *Health affairs*, 12(2):164–76, Jan. 1993.

[60] R. A. Santarella, G. Skiniotis, K. N. Goldie, P. Tittmann, H. Gross, E.-M. Mandelkow, E. Mandelkow, and A. Hoenger. Surface-decoration of microtubules by human tau. *Journal of molecular biology*, 339(3):539–53, June 2004.

[61] N. Shahani and R. Brandt. Functions and malfunctions of the tau proteins. *Cellular and molecular life sciences : CMLS*, 59(10):1668–80, Oct. 2002.

[62] R. Skrabana, J. Sevcik, and M. Novak. Intrinsically disordered proteins in the neurodegenerative processes: formation of tau protein paired helical filaments and their analysis. *Cellular and molecular neurobiology*, 26(7-8):1085–97, 2006.

[63] J. P. Snyder, J. H. Nettles, B. Cornett, K. H. Downing, and E. Nogales. The binding conformation of Taxol in beta-tubulin: a model based on electron crystallographic density. *Proceedings of the National Academy of Sciences of the United States of America*, 98(9):5312–6, Apr. 2001.

[64] S. Tahirovic and F. Bradke. Neuronal polarity. *Cold Spring Harbor perspectives in biology*, 1(3):a001644, Sept. 2009.

[65] R. Y. Tsien. The green fluorescent protein. *Annual review of biochemistry*, 67:509–44, Jan. 1998.

[66] S. Uppuluri, L. Knipling, D. L. Sackett, and J. Wolff. Localization of the colchicine-binding site of tubulin. *Proceedings of the National Academy of Sciences of the United States of America*, 90(24):11598–602, Dec. 1993.

[67] L. C. Walker, M. I. Diamond, K. E. Duff, and B. T. Hyman. Mechanisms of protein seeding in neurodegenerative diseases. *JAMA neurology*, 70(3):304–10, Mar. 2013.

[68] J.-z. Wang and F. Liu. Microtubule-associated protein tau in development, degeneration and protection of neurons. *Progress in neurobiology*, 85(2):148–75, June 2008.

[69] C. Weissmann and R. Brandt. Mechanisms of neurodegenerative diseases: insights from live cell imaging. *Journal of neuroscience research*, 86(3):504–11, Feb. 2008.

[70] C. Weissmann, H.-J. Reyher, A. Gauthier, H.-J. Steinhoff, W. Junge, and R. Brandt. Microtubule binding and trapping at the tip of neurites regulate tau motion in living neurons. *Traffic*, 10(11):1655–68, Nov. 2009.

[71] H. Witte and F. Bradke. The role of the cytoskeleton during neuronal polarization. *Current opinion in neurobiology*, 18(5):479–87, Oct. 2008.

[72] H. Witte, D. Neukirchen, and F. Bradke. Microtubule stabilization specifies initial neuronal polarization. *The Journal of cell biology*, 180(3):619–32, Feb. 2008.

Abbreviations

μ ..... micro-

k_{off} ..... Dissociation rate

k_{on} ..... Association rate

k^*_{on} ..... Apparent association rate

% (v/v) ..... percent by volume

% (w/v) ..... percent by weight

Aβ ..... Amyloid β peptide

AD ..... Alzheimer’s disease

APP ..... Amyloid precursor protein

Asp ..... Aspartate

bp ..... basepairs

c ..... centi-

c-terminal ..... carboxyterminal

D ..... Diffusion coefficient

d (Prefix) ..... deci-

Da ..... Dalton

DMSO ..... Dimethylsulfoxid

DNA ..... Desoxyribonucleic acid

EpoD ..... Epothilone D

FDAP ..... Fluorescence decay after photo activation

g ..... gram

GFP ..... Green fluorescent protein

Gly ..... Glycine

H (Amino acid) Histidine

HRP ..... Horse raddish peroxidase

k ..... kilo-

M ..... molar = *mol*/l

m (Prefix) ..... milli-

m (Suffix) ..... meter

MAPs ..... Microtubule-associated proteins

mCherry ..... Monomeric Cherry

n ..... nano-

NFTs ..... Neurofibrillary tangles

NGF ..... Nerve growth factor

p ..... pico-

PAGFP ..... Photoactivatable green fluorescent protein

PC12 ..... Pheochromocytoma

PCR ..... Polymerase chain reaction

PVDF ..... Polyvinylidene fluoride

R ..... Repeat region in tau sequence

rpm ..... Rounds per minute

s ..... second

SDS ..... Sodium dodecyl sulfate

Ser ..... Serine

T (Amino acid) . Threonine

Tyr ..... Tyrosine

UV ..... Ultraviolet

V ..... Volt

wt ..... Wild type

7 Curriculum Vitae

Name	Jörg Helmut Brühmann
Adress	Mittelstraße 3 49074 Osnabrück
Contact	joerg.bruehmann@biologie.uni-osnabrueck.de
Birthday	28th of January, 1984
Place of Birth	Regensburg, Bavaria, Germany
Education and study	
2011-2014	Doctoral thesis in the department of Neurobiology at the University of Osnabrück. Topic: "Interaction of tau protein with microtubules in neural cells"
2007-2011	Studies of biology at the University of Osnabrück Degree: Diplom-Biologe Topic: "Einfluss von Proteindomänen auf die Mobilität von humanem Tau-Protein in neuralen Zellen"
2004-2007	Studies of biology at the University of Regensburg Degree: Intermediate diploma
Military service	
2003-2004	9 months of military service, 3./Fernmeldebataillon 4 in Regensburg
School education	
1994-2003	Werner von Siemens Gymnasium Regensburg Aquirement of the general qualification for university entrance
1990-1994	Grundschule Pettendorf-Pielenhofen

8 Eidesstattliche Erklärung

Ich erkläre hiermit, dass ich die vorliegende Arbeit ohne unzulässige Hilfe Dritter und ohne Benutzung anderer als der angegebenen Hilfsmittel angefertigt habe. Die aus anderen Quellen direkt oder indirekt übernommenen Daten und Konzepte sind unter Angabe der Quelle gekennzeichnet.
Bei der Auswahl und Auswertung folgenden Materials haben mir die nachstehend aufgeführten Personen in der jeweils beschriebenen Weise entgeltlich / unentgeltlich geholfen.

1. Herr Maxim Igaev hat die Skripte für das Modeling und Fitting erstellt und die Errechnung der Parameter k^*_{on} und k_{off} (Abschnitt 3.2.4.3) für alle Bedingungen und der daraus abgeleiteten "Bound"-Werte durchgeführt.

2. Herr Maxim hat die Auswertung für Abbildung 4.13 durchgeführt.

Weitere Personen waren an der inhaltlichen materiellen Erstellung der vorliegenden Arbeit nicht beteiligt.
Insbesondere habe ich hierfür nicht die entgeltliche Hilfe von Vermittlungs- bzw. Beratungsdiensten (Promotionsberater oder andere Personen) in Anspruch genommen. Niemand hat von mir unmittelbar oder mittelbar geldwerte Leistungen für Arbeiten erhalten, die im Zusammenhang mit dem Inhalt der vorgelegten Dissertation stehen.
Die Arbeit wurde bisher weder im In- noch im Ausland in gleicher oder ähnlicher Form einer anderen Prüfungsbehörde vorgelegt.

(Ort, Datum, Unterschrift)

9 Acknowledgments

First, I would like to thank Prof. Dr. Roland Brandt for giving me the opportunity to work in his department for the last four years, for giving me the chance to do this work and for supporting me over the past years in which I learned so much.
I would like to thank Prof. Dr. Christian Ungermann for being second reviewer on this thesis. Also I'd like to thank Prof. Dr. Günter Purschke and Lidia Bakota for taking part in the board of examiners.
I would really like to thank all present and former members of the department of neurobiology! Thank you, Anne, for helping me with my fist steps as PhD student. Thank you, Fred, for all the serious and not so serious conversations - it meant a lot to me. Thank you, Henning, for the good times on summer parties and all all the smalltalk. Thank you Maxim for helping me with all the maths. Thank you, Lidia for helping me with all the mouse preparation work. Thanks to all I forgot to mention separately, be sure it was not my intention to exclude you from this acknowledgment ;). Thanks to all you neurobiologists for nice conversations, breakfasts, works outings and a lot of fun!
I would like to thank all my friends here in Osnabrück, for being on my side for the past seven years here in northern Germany - hey, it's far away from home, ya know? Thanks for all the fun we had during that time and for the feeling that I never was alone. I would also like to thank my friends back in Regensburg for abiding by me and for constantly asking when I will come back home.
Thank you, Sven, for answering all the questions I had about theses, jobs etc. and for your support with all that.
Many thanks to my parents for their support during all that time, for that you believed in me since the time I started studying and then doing my PhD. Thank you for letting me know that I always could count on you.
Thank you, Nina, for being by my side during the last few months of this work and for helping me keep my sanity.
Thanks to whoever is responsible for that little portion of luck that helped me through from time to time and to whoever provided the bad luck: HA! I made it anyway!
Well, that's it. When this goes to print, my time as a PhD student goes to an end. Time to start something new. Bye bye!

Notes